Marine and Petroleum Geology 171 (2025) 107172

Contents lists available at ScienceDirect

Marine and Petroleum Geology

journal homepage: www.elsevier.com/locate/marpetgeo

Structural evolution of the Handun salt diapir, Zagros fold and thrust belt, southern Iran

Marco Snidero [*], Josep Anton Muñoz, Pablo Santolaria, Nuria Carrera, Mireia Butille

Institut de Recerca Geomodels and Departament de Dinàmica de la Terra i de l'Oceà, UB (University of Barcelona), Spain

ARTICLE INFO

Keywords:
Eastern Fars
Salt tectonics
Halokinetic sequences
Balanced cross-section
Hormuz salt
Welding
Thin-skin
Basement

ABSTRACT

The Fars region, in the Zagros fold and thrust belt, hosts a wide range of diapirs piercing over 10 km of stratigraphic sequence. Comprising Precambrian to Early-Cambrian Hormuz Salt, these diapirs exhibit a prolonged history of evolution. Outcrop evidence for understanding the diapir deformation history is mostly limited to the Cenozoic contractive phase, and the seismic data lacks the necessary quality for an exhaustive understanding of the deepest structure's geometries. Through regional and field evidence we unravel the Handun salt structure evolution and propose a sequential restoration to describe the key deformational events. Our study presents a field-based novel regional balanced cross-section and a 3D-geological model, and addresses the role of structural inheritances and the position of the Handun diapir with respect to the decupled basement. The performed field studies describe folds and unconformities related to Cenozoic halokinetic sequences with exceptional clarity. It was possible to observe changes of the diapir activity along the structure and provide field evidence for the relative timing and kinematics of primary and secondary welding. Finally, our data suggest that the Handun diapir formed in the early Paleozoic above the shoulder of a basement extensional fault, and was partially translated above its southern hanging-wall during the shortening. In the Paleocene a sustained ratio of salt rise rate was enhanced by the Zagros/Oman contraction. In response to the Oligocene continental collision, the diapir was profusely supplied with salt, which flared upward to form overhangs. Since the middle Miocene the salt supply slowly depleted, with the diapiric walls remaining near the surface but tapering upward, probably due to primary welding or increased sedimentation. Secondary welding occurred post-Pliocene in the last stages of the diapir evolution with consequent development of a secondary minibasin.

1. Introduction

The Eastern Fars is an exceptional natural laboratory for the study of salt structures. There, the Precambrian to Early-Cambrian Hormuz Salt forms numerous diapirs cropping out in different structural positions, from the hinterland to the offshore undeformed foreland of the Zagros fold and thrust belt and the Oman Ranges (Fig. 1) (e.g., Richardson, 1926; De Böckh et al., 1929; Lees, 1931; Harrison, 1931; Kent, 1958; Gansser, 1960; Stöcklin, 1968; Player, 1969; Falcon, 1969; Perotti et al., 2016). As in many other fold and thrust belts, shortening decreases forelandwards, consequently diapirs in the hinterland are more squeezed than those found offshore, along the undeformed foreland (e.g., Davis et al., 1983; Santolaria et al., 2021). Onshore, only the Cenozoic and, rarely, Mesozoic rocks crop out in close contact with the Hormuz Salt (Fig. 1) which permits the observation of the interplay between their growth with the host rock and interpret their Mesozoic to Cenozoic evolution. Offshore, subsurface data provides insights into the geometry of structures at depth, allowing for a better interpretation of the Paleozoic and Mesozoic diapiric evolution (Alsouki et al., 2011; Ezati Asl et al., 2019; Hassanpour et al., 2021; Perotti et al., 2016; Snidero et al., 2020).

In this structural and stratigraphic setting, understanding the long-lived diapirism deformational history of the eastern Fars region requires observations at various scales, employing different analogs, and adopting a regional perspective to depict the overall picture of diapir evolution.

There is a widespread consensus about the fact that there was a continuous diapiric exposure of the Hormuz Salt since the early Paleozoic, indicating passive growth since then (Jahani et al., 2009; Perotti et al., 2016; Snidero et al., 2020). However, the structural setting and the interpretation of the pre-Hormuz Salt basement architecture remain speculative, as does the role of basement deformation in diapirism. In

* Corresponding author.
E-mail address: msnidero@ub.edu (M. Snidero).

https://doi.org/10.1016/j.marpetgeo.2024.107172
Received 17 April 2024; Received in revised form 14 October 2024; Accepted 20 October 2024
Available online 22 October 2024

some diapirs, the presence of basement faulting influencing the structural location of diapirs has been suggested (Hassanpour et al., 2021; Jahani et al., 2017), but clear evidence is just available in the northern Persian Gulf (Stewart, 2017), where several diapirs are located on the shoulder of basement normal faults. Previous interpretations of the Mesozoic and Cenozoic evolution of diapirs are largely based on novel field observations that reveal halokinetic sequences and distribution of depocenters in close contact to diapirs (Snidero et al., 2019; Faridi et al., 2021; Adineh et al., 2024). These evidences indicate a long-lasting diapiric passive growth stage (Paleozoic-Lower Cretaceous), followed by the contractional reactivation of salt structures (Late Cretaceous onwards) (e.g. Ezati Asl et al., 2019; Hassanpour et al., 2021; Snidero et al., 2020). Such diapiric contraction led to diapir rejuvenation and squeezing (e.g., Callot et al., 2007; Santolaria et al., 2021a, 2021b).

In summary, due to the limited subsurface data available, it is still unclear to what extent the basement-involved structures beneath the Hormuz Salt played a role in the diapiric evolution. Additionally, despite the aforementioned contributions, only a few structures have been subjected to detailed field studies, with most interpretations focusing on specific time intervals. To address these gaps, we bring regional and local evidences together with field analogs to propose a deformation history for the Handun salt structure and its relationship with the underlying basement.

The doubly-plunging Handun anticlinal lies in the eastern area of the Fars region, where the southeastern termination of the Zagros fold and thrust belt, displays a clear shift in structural alignment. The prevailing NW-SE-trending Zagros hinterland structures, including the Main Zagros fault, changes gradually to the N-S-trending Zendan fault and the NNE-SSW-trending Oman Ranges (Fig. 1). This geometry also delineates the extent of the Precambrian to Early Cambrian Hormuz evaporitic basin, suggesting a pre-existing basement architecture marked by normal faulting and shaped by earlier tectonic events (Fig. 2) (Koop and Stonley, 1982; Husseini and Husseini, 1990; Snidero, 2021).

The Handun anticline itself exhibits a particular asymmetry where frontal and back limbs are vertically offset approximately 2 km with respect to the top of the basement. Such structural offsets are not exclusive to the Handun structure and different interpretations have been proposed for their origin (Leturmy and Robin, 2010). Limited data on the Paleozoic sequence poses a significant challenge in understanding the role of the basement-involved structures in these positive structural offsets (Hinsch et al., 2022). Consequently, uncertainties regarding total stratigraphic thickness become a primary concern. These uncertainties, which have already been summarized by Hinsch and choauthors (2022), lead to ambiguous interpretations, with some studies proposing both thin- (e.g., Hinsch et al., 2022; Jahani et al., 2009). and thick-skinned (e.g., Alavi, 2007; Molinaro et al., 2005; Tavakoli et al., 2013) structural styles for the same area (e.g., Alavi, 2007; Molinaro et al., 2005; Jahani et al., 2009; Tavakoli et al., 2013.

In this work, we delve into the implications of this structural feature by balancing a regional cross-section and presenting a 3D elevation model of the Oligocene pre-folding horizon, taking into account potential influences from both basement and salt-related inherited structures. Using regional sections firstly assist in delineating the geometry of the basal detachment and identifying structural offsets. Furthermore, the three-dimensional representation of these features is crucial for minimizing uncertainty when interpreting deep-seated basement structures.

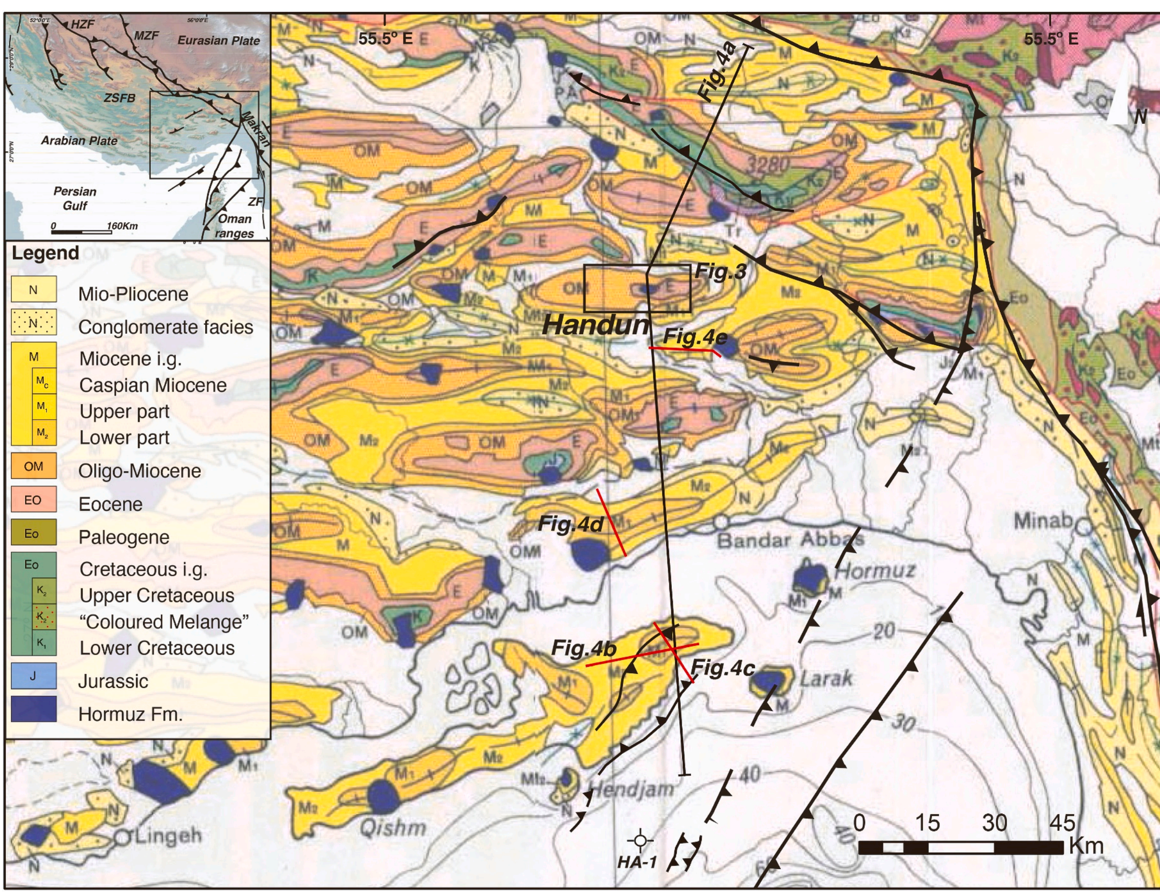

Fig. 1. 1:2,500,000 Geological map compiled by NIOC, showing the major structural elements of the southeastern Zagros fold and thrust belt in the eastern Fars Region. The regional cross section, and wells used are located in the main map. Inset map: Illustration of the major structural elements at a regional scale. ZSFB: Zagros Simply Folded Belt, HZF: High Zagros Fault, MZF: Main Zagros Fault, ZF: Zendan Fault (Falcon, 1969). The inset basemap was created using the Shuttle Radar Topography Mission dataset (Farr et al., 2007).

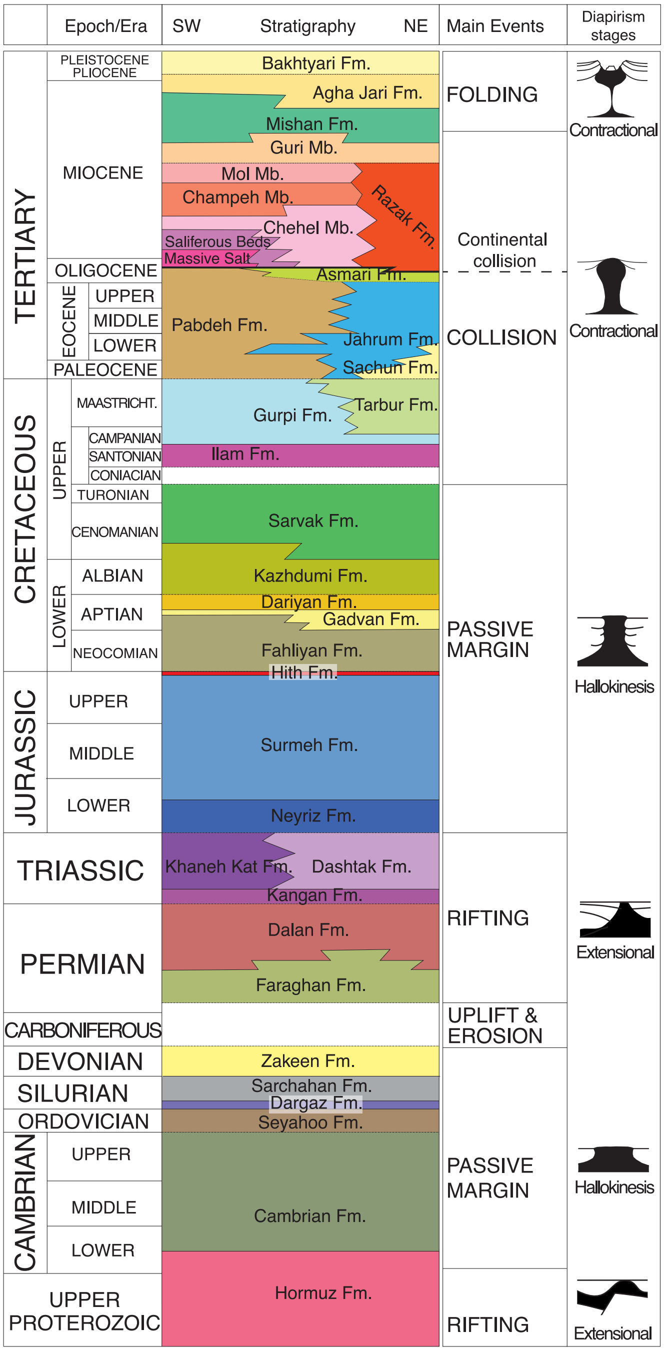

Fig. 2. Stratigraphic chart of the eastern Fars region. Main tectonic events and possible mechanisms for the salt deformation in the area are showed. The bolted line at the top of the Asmari Fm. represents the selected horizon reconstructed in the 3D model. (Modified from James and Wynd, 1965; Searle et al., 2014; Pirouz et al., 2015; Snidero et al., 2019).

The outstanding exposure of the Handun diapir and the exceptional outcrop conditions of the Cenozoic sequence provide clear insights into the geometric and stratigraphic relationship between the Paleogene to Pliocene overburden and the Hormuz Salt (Faridi et al., 2021). Field evidence allowed us to go a step further into the understanding of the occurrence, timing, and kinematics of primary and secondary welding in relation to Cenozoic diapir growth and delineate diapir evolution across spatial dimensions.

2. Tectonostratigraphy

The Handun anticline is situated in the Eastern Fars, 30 km south of the High Zagros Fault, the thrust structure representing the northern limit of the Simply Folded Belt within the Zagros Fold and Thrust Belt (Falcon, 1969) (Fig. 1).

At the base of the over 10 km of stratigraphic sequence, the crystalline basement consists of a Precambrian Gondwana terrain, which was dismembered during the break-up of Gondwana at the end of the Neoproterozoic (c. 570-530 Ma) along both N-S and E-W-trending basement faults, (Stoesser and Camp, 1985; Beydoun, 1991; Husseini, 2000) (Fig. 2). Within the study area, the Gondwana break-up led to the development of NW-trending left-lateral strike slip faults and NE-trending breakaway faults, referred to as the Najd Rift System (Husseini, 2000). This tectonic evolution led to the deposition of the Hormuz Salt, with these Neoproterozoic fault systems delineating the segmentation of the Hormuz Salt basin (Husseini, 1988). The Hormuz Salt is composed by a sequence of massive halite, anhydrite, limestones, dark dolomites and some red sandstones and shales (Kent, 1970).

Following the Gondwana breakup, a relatively stable passive margin developed during the early Paleozoic. The Late Devonian witnessed diffuse extensional deformation accompanied by significant uplift, attributed to either thermal effects (Tavakoli et al., 2013) or the far-reaching effects of the Hercynian Orogeny (Faqira et al., 2009). This phase resulted in erosion and peneplanation (Frizon de Lamotte et al., 2013).

Most of the sequence from Ordovician up to the Devonian is made up of epicontinental siliciclastics deposited in an intracratonic setting (Ghavidel-Syooki et al., 2014). By the end of the Devonian, general subsidence facilitated the development of a Carboniferous/Permian sag basin (Frizon de Lamotte et al., 2013).

During the Late Permian-Early Jurassic, rifting between the Arabian and Cimmerian terrains led to the formation of the Neo-Tethys Ocean (Berberian and King, 1981; Koop et al., 1982; Tavani et al., 2018). The Neo-Tethys rifting event led to the accumulation of a basal sequence of red beds (Faraghan Fm.), overlain by the bioclastic limestones and dolomites of the Dalan Fm. (Alavi, 2004; Zamanzadeh et al., 2009) (Fig. 2). The Triassic sequence consists of a succession of northeastward prograding, interbedded evaporites, and dolomites with interlayered shallow-marine limestones northward (Kangan Fm., Dashtak Fm. and Khaneh Kat Fm.) (Fig. 2). On top, an unconformity related to the Neo-Tethys opening, separates it from the overlying Jurassic to Cretaceous continental shelf deposits (Alavi, 2004).

Subsequently, in the Upper Jurassic-Lower Cretaceous, the Arabian plate's northeastern margin (including the current Zagros region) remained tectonically quiescent.

The lowermost Jurassic to upper Turonian strata were accumulated mostly on a shallow continental shelf, facing north and northeast towards the Neo-Tethys Ocean. The Neyriz Fm. (Lower Jurassic) is composed of three distinct units: the lower unit primarily features thin-bedded dolomites and green shales, the middle unit is characterized by sandy silts, and it is overlain by a more argillaceous thin-bedded limestones transitioning to mudstones unit (James and Wynd, 1965). The Surmeh Fm. (Middle to Upper Jurassic) consists of normal marine, micritic limestones, often chalky and pyritic (Bowe, 1976) now extensively dolomitized. The Jurassic sequence ends with the Hith Fm. made by anhydrite in supertidal sebkha environments (Fig. 2). The base of the lower Cretaceous succession consists of a deep-water chalky or argillaceous limestone transgressive unit (Fahliyan Fm.) overlain by light gray marls interbedded with cryptocrystalline limestones deposited from the Barremian to early Aptian (Gadvan Fm.), suggesting that basinal depositional conditions persisted till Aptian time when a regressive unit interbedded with pellet oolitic beds was deposited (Dariyan Fm.) and overlain by the Albian thin marly unit of the Kazhdumi Fm. deposited during the Albian. The shallow depositional environment persisted until Santonian times with the deposition of a thick carbonatic platform

(Sarvak and Ilam Fms.) (Fig. 2).

During the Late Cretaceous to Cenozoic, oblique convergence between the Arabian and Eurasian plates led to the closure of the Neo-Tethys Ocean and the subsequent continental collision that formed the Oman and Zagros belts (e.g., Stöcklin, 1968; Ricou et al., 1977; Berberian and King, 1981; Alavi, 2007; Barrier and Vrielynck, 2008; Agard et al., 2005, 2011; Vergés et al., 2011; Mouthereau et al., 2012; Orang et al., 2017). This phase culminated with the obduction of ophiolite thrust sheets along the northeastern Arabian continental margin (Coleman, 1981; Alavi, 2007; Searle et al., 2014), and the local development of "proto-Campanian-Maastrichtian" foreland basins (Ziegler, 2001; Alavi, 2004; Saura et al., 2011).

The first contractional deformation is coeval with the deposition of the transgressive lower marly unit of the Gurpi Fm. during the Campanian-Maastrichtian, overlain by the Tarbur Fm. regressive limestone (Fig. 2). During the Paleocene, Eocene, and part of the Oligocene, the foreland basin is infilled by a thick succession of marls represented by the Pabdeh Fm (Rezae, 2014). This formation grades progressively into the carbonate sequence of the Jahrum Fm. northward, which is ultimately replaced by the Sachun Fm. underneath the upper part of the Jahrum carbonates (Fig. 2).

The onset of continental collision between the Arabian and Central Iranian microplates took place from the late Oligocene to the early Miocene (Stoneley, 1981; McQuarrie et al., 2003; Agard et al., 2005; Mouthereau et al., 2012; Khadivi et al., 2012; McQuarrie and van Hinsbergen, 2013). This convergence persisted until recent times, leading to the development of the Zagros fold and thrust belt and the associated Persian foreland basin (e.g., Molinaro et al., 2005; Mouthereau et al., 2007).

The contractional onset is regionally represented by sediments of the Asmari Fm., a marine carbonate unit which transgressed the Jahrum limestones (Fig. 2). In the Handun structure, part of the Oligocene up to the middle Miocene sequence, corresponds to the sandy marls and red beds of the Razak Fm.

The period above the middle Miocene is characterized by a rapid, conformable transition to the resistive limestones of the Guri Fm. (Fig. 2). It consists of hard, creamy and fossiliferous limestones interbedded with rubbly limestones and marls (Rahmani et al., 2010). Mishan Fm. (mid to late Miocene), which overlies the Guri Mb., is a sequence of shallow-water marine marls interbedded with bioclastic limestones and occasionally thin bioclastic sandstones.

The clastic Agha Jari and Bakhtyari Fms. deposit synchronously with Pliocene folding of the Simply Folded Belt of the Fars province (Fig. 2). The Aghajari Fm. (Late Miocene to Pliocene) consists of gray to brown calcareous sandstones, siltstones, silty marls and occasional sandstone beds, and shelly limestones (Bozorgnia and Agah, 1973). Bakhtyari Fm. is made of massive and thick-bedded, coarsening upwards fluvial deposits, consisting of polymictic conglomerates, cross-bedded sandstones, siltstones, and shales.

3. Datasets and methods

This work integrates subsurface and surface data coming from different surveys and techniques including seismic reflection profiles, well data, geological mapping, and structural measurements. The datasets at our disposal include.

i) Onshore and offshore 2D seismic reflection data. The off-shore survey includes an area of 34,000 km^2 in the Persian Gulf, proximate to the Hormuz Strait. This survey features an orthogonal grid configuration with 2 km spacing and a maximum recorded depth of 7 s (two-way time). Onshore surveys exhibit an uneven distribution, orientation, and spacing, primarily clustered around key structures, especially along the coastline and within Qeshm Island. Seismic data quality tends to be favorable for offshore lines, but variable for onshore surveys, with many structures inadequately imaged. The onshore-offshore correlation involved shifting onshore data of from datum 900 m to datum 0, followed by iterative refinement for each line, utilizing topography as a reference. Refer to Fig. 4 for the seismic reflection profiles used to constrain the regional balanced cross-section.
ii) Interpretation of seismic data was supplemented with insights from 24 exploration wells (locations in Fig. 5). These wells attain a maximum depth of 4625 m and provide information on thicknesses and lithologies through the Permian sequence.
iii) Over 1600 dip measurements from field campaigns, combined with more than 1500 dips (Snidero, 2023), obtained through digital mapping (e.g., Tavani et al., 2011; Snidero et al., 2011), leveraging using a 30 m (ASTER) Global Digital Elevation Model and high-resolution satellite imagery.
iv) Existing geological maps of the complete study area at diverse scales (1:250,000, 1:100,000, and 1:50,000), along with associated dip data. These maps, in conjunction with supplementary mapping efforts, facilitated the synthesis of the geological map illustrated in Fig. 3.

These datasets are integrated as constraints in constructing both the Faraghun-Hulur regional cross-section (Fig. 4) and the 3D elevation model (Fig. 5) and together, illustrate the overarching structural framework of the studied region.

The cross-section was built following the dip domain technique (e.g., Coates, 1945; Gill, 1953; Suppe, 1985; Groshong, 2006; Carrera et al., 2006; Snidero et al., 2011). A flexural slip model was applied to unfold the non-evaporite units, aiming to conserve line lengths and areas (e.g., Dahlstrom, 1969; Mitra, 1992; Rowan, 1993; Marshak and Woodward, 1988). The area of the salt layer was preserved with the exception of minor out-of-plane movements related to salt flow and diapiric salt extrusions.

The 3D elevation model represents the top of the Asmari Fm. and its Oligocene lateral equivalents. The methods employed for the onshore 3D surface reconstruction are based on the fundamental concepts used for the regional cross-section, while accounting for all available data and their precise positions (Langenberg et al., 1987; Groshong, 2006; Carrera et al., 2006). By minimizing projection errors, a 3D vector field was defined, composed of domains featuring constant plunge values. To ensure accuracy of the 3D vector field, dip data was subdivided into approximately 250 cylindrical domains, each with a specific axis orientation (plunge lines). The axial planes between different plunge domains, along with their positioning, completes the integral structural framework needed for the 3D reconstruction of the Asmari surface, following the methodological steps proposed by Carrera et al. (2006). The plunge lines resulted from the structural analysis have been anchored to the bedding surface traces, to the regional cross-section and to the wells markers. Finally, using this geometrical framework, we interpolated the Asmari reference surface using the Discrete Smooth Interpolation algorithm (Mallet, 1992).

In contrast, the offshore 3D model was entirely constrained by seismic interpretation tied to exploration wells. Finally, the onshore and offshore reconstructed surfaces were seamlessly integrated to result in a comprehensive, unified surface for the entire study area.

4. Faraghun-Hulur regional cross-section

The section trace as shown in Fig. 1 was strategically chosen to intersect well-exposed geological structures, from north to south, including the Faraghun, Finu, Handun, West Namak, Genu, Suru, and Zirang-Hulur. Broadly, these structures can be classified as detachment anticlines (faulted in some cases) that are flanked by wide, flat-bottomed synclines. On a regional scale, there is no prevalent vergence, and the taper angle remains low (Fig. 4a). The position of the anticlines aligns with the presence of pre-existing salt diapirs and there is not a consistent

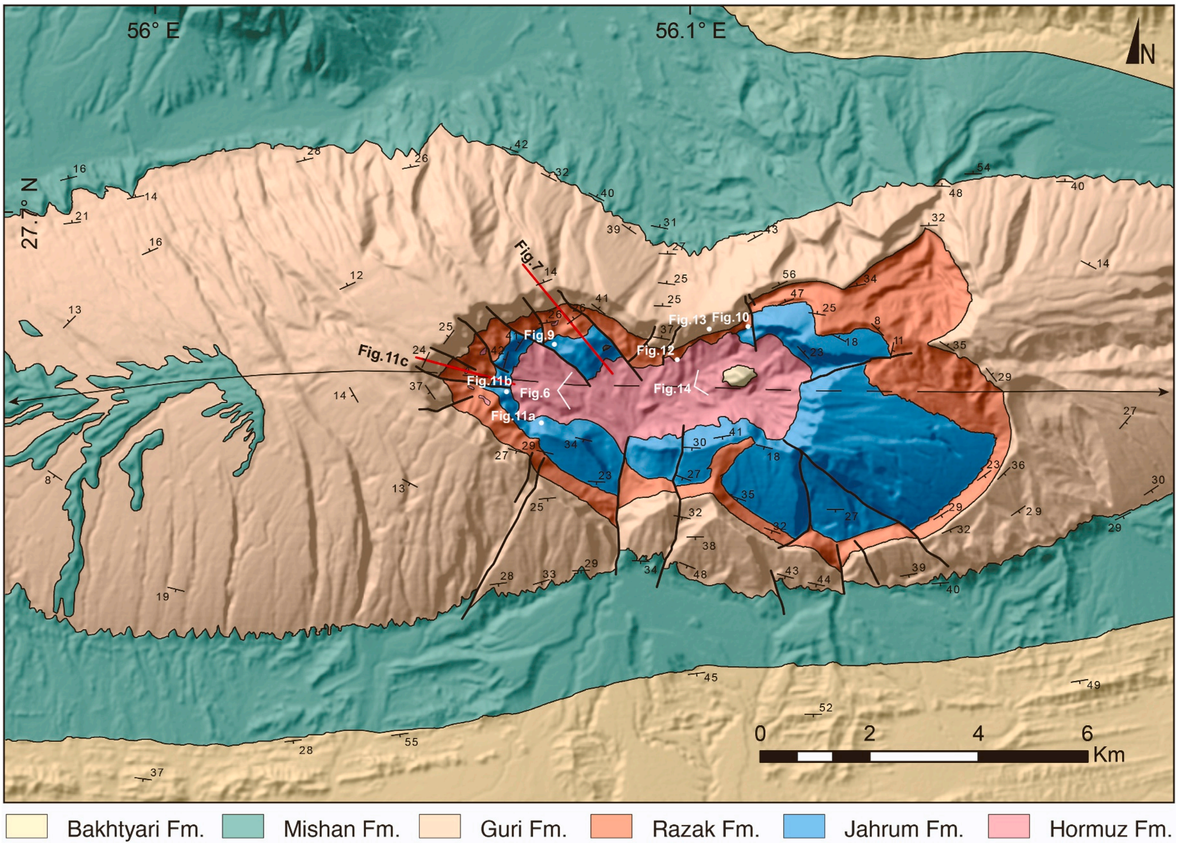

Fig. 3. Geological map of the Handun structure (location in Fig. 1). Notice patches of the Hormuz Salt outcropping within the Razak Fm. around the diapir.

pattern of structural spacing or wavelength. Additionally, the irregular distribution of detachment anticlines suggests a primary influence from the locations of pre-existing salt structures.

We defined the base of the synclines as regional markers for correlating the regional detachment horizon. To the north of the Genu Anticline, the basal detachment progressively tilts towards the internal segments of the mountain range (northwards) (Fig. 4a). On the other hand, to the south of the Genu structure and towards the deformation front of the Zagros fold and thrust belt, there is a progressive increase in stratigraphic thickness from 150 m to over 4 km within the upper Cretaceous to Paleocene sequence (Fig. 4a, b and c). This change in the stratigraphic record is associated with the foreland development of the NE-SW-trending Oman Ranges (Searle et al., 2014; Orang et al., 2017; Snidero, 2021), indicating NW-related lithospheric flexure, which consequently influences the dip of the regional detachment.

The selected cross-section shows this bimodal structural flexure: one near the Persian Gulf to the south, and another extending broadly to the north within the Zagros Mountains (Fig. 4a). This bimodal flexure contrast the cross-section of Jahani et al. (2009) who proposed a consistent deepening of the basement towards the north. It underscores the interplay between the Zagros-related structures to the north and their connection to Oman-related structures.

The stratigraphic thicknesses above the Hormuz Salt exhibit variations along the section. Among these, the thickness of the Paleozoic succession is the primary source of uncertainty. To address this uncertainty, we have utilized field measurements from exposed units within the Faraghun structure, spanning from the Ordovician to the Permian. Additionally, we have incorporated thickness data from previous studies (Saberi et al., 2016), particularly for the Cambrian units. In cases where the sequence is well-preserved, the Paleozoic succession attains a minimum thickness of 4500 m.

However, variations in thickness arise notably at the positions of inferred pre-existing salt structures and associated minibasins, which are considered active since Paleozoic times (Jahani et al., 2009; Perotti et al., 2016; Snidero et al., 2020).

The Triassic sequence exhibits a thickness range, spanning from 640 m (drilled in the Finu and Namak wells) to a maximum of 1800 m in the southern and northern portions of the section. The distribution of Triassic depocenters, as revealed by seismic and well datasets, follows the trend of the innermost structures within the Zagros and Oman chains, exhibiting a similar distribution pattern. The thickness of the Jurassic to Turonian sequence attains a maximum of 1520 m in the well Finu-1, exhibiting notable variations likely associated with salt movement during the development of the Arabian passive margin (e.g. reaching over 2300 m in the well Bostaneh). The upper Cretaceous and Paleogene sequences are well-exposed in the field (Fig. 1) and have been confidently interpreted in seismic profiles. Thicknesses reveal a trend of thickening towards the south and north, ranging from a few hundred meters in the center of the section to over 2500 m at the edges (Fig. 4a). Notably, a distinct and abrupt thickening shift of 2 km is observed from the southern to the northern limb of the Faraghun structure. These substantial variations in thickness coincide with the timing of convergence and the development of foreland basins. Miocene to Pliocene depocenters are notably influenced by folding caused by the shortening of the Zagros orogen, leading to thickness variations ranging from a few hundred meters in the anticline crests to over 4 km in the synclines (Fig. 4a).

In addition to these regional considerations, a detailed examination of each individual structure reveals key deformational characteristics within the area. Starting from the southern end, the Zirang-Hulur anticlines is interpreted to be cored with Hormuz Salt, overlain by a lower Cretaceous to Pliocene sequence. This anticline is bounded by a second-order, south-directed thrust that affects the base of the Gurpi sequence. Another northwestward-directed thrust cuts through the Pabdeh Fm. In

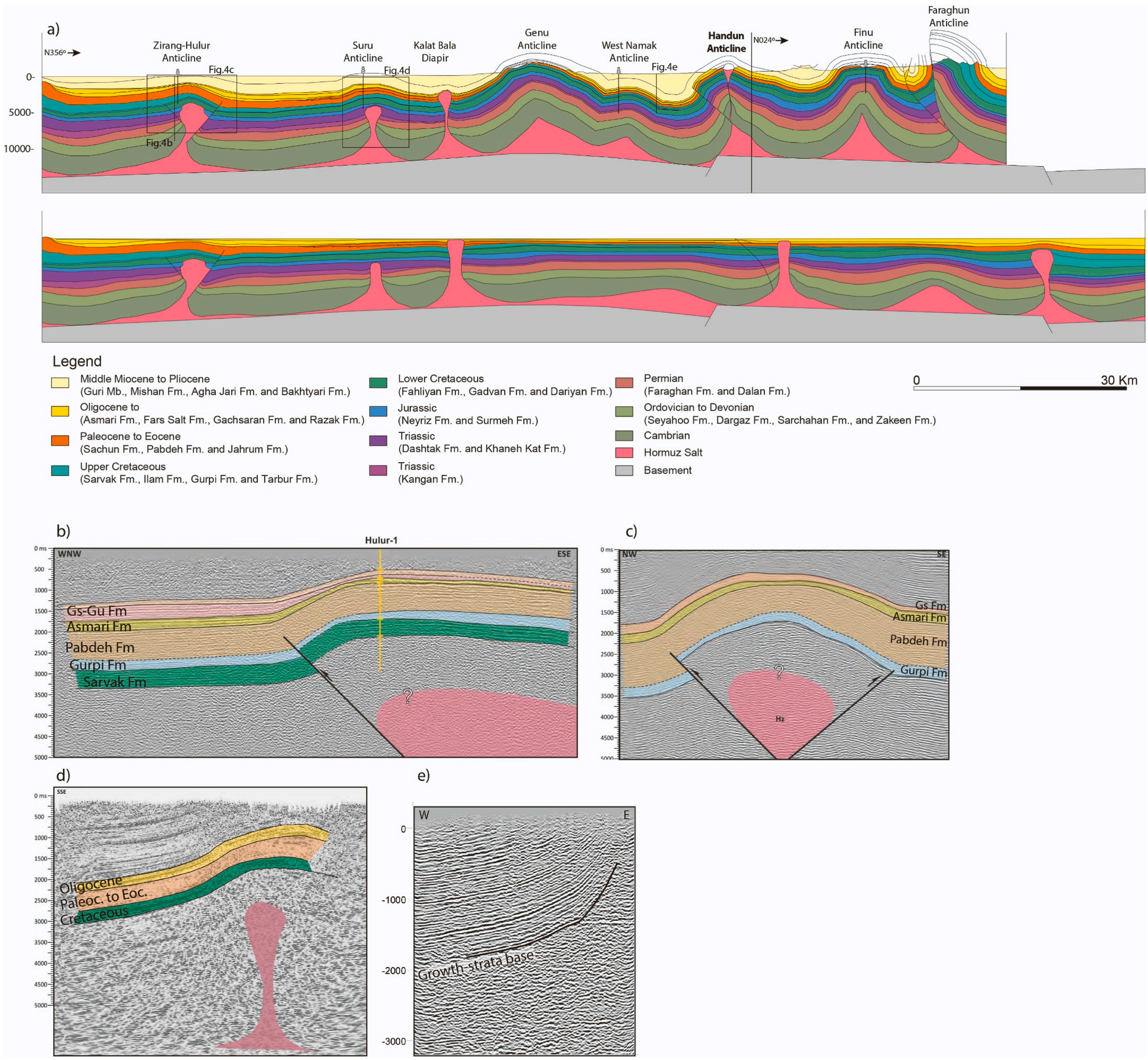

Fig. 4. a) Above, the balanced regional cross-section passing through the Handun Anticline. Below, the cross-section is restored at the deposition of the Mishan Fm. Black square indicate the location for the interpreted seismic lines. b) and c) Seismic lines across the Zirang-Hulur anticline. This anticline is cored by Hormuz Salt and bounded by a NW-directed thrust and a SE-directed second-order backthrust. The main thrust dies out within Pabdeh succession. d) Seismic lines along the Suru anticline. e) E-W-trending seismic line to the south of the Handun anticline, depicting the base of a thick package of syn-folding growth-strata thinning toward the Namak anticline. (Locations in Fig. 1).

map view (Fig. 1), the faults bounding the Zirang-Hulur anticlines die out westwards, where the periclinal closure of the NW-SE-trending Gavarzin anticline intersect with. Close to the base of the anticline, the Gurpi Fm. thins against the anticlinal crest, while the Pabdeh Fm. exhibits thickness changes across the main thrust fault. The Asmari Fm., extending at least up to the Gachsaran Fm., exhibits growth strata and geometries that pinch out against the fold limbs. Despite the seismic image not being optimal (Fig. 4b and c), the Guri carbonates display no discernible thickness changes across the structure, implying that the process of fold growth might have ceased at this point. Overall, the interpretation suggests that the anticline began developing during the deposition of the Gurpi Fm., experienced peak folding activity during the Pabdeh Fm. deposition. The process included thrust development and continued fold growth through the deposition of the Asmari and Gachsaran Fms., ultimately stopping before the Guri Mb. deposition. Nevertheless, the folded configuration of the Guri Mb., extending up to recent deposits, indicates a more recent phase of reactivation.

To the north, ~15 km-wide syncline separates the Zirang-Hulur anticlines from the subsequent structure, the Suru anticline. This particular anticline is clearly visible in seismic data and shares characteristics of being cored by Hormuz Salt, as indicated by distinctive semi-transparent seismic facies (Fig. 4d). The anticline's rounded hinge and gently sloping limbs corroborate this interpretation, further supported by the presence of a Hormuz Salt diapir at its western closure. The thickening of the Triassic sequence toward the diapir suggests the folding of a pre-existing rim syncline. In contrast, the thickening of the

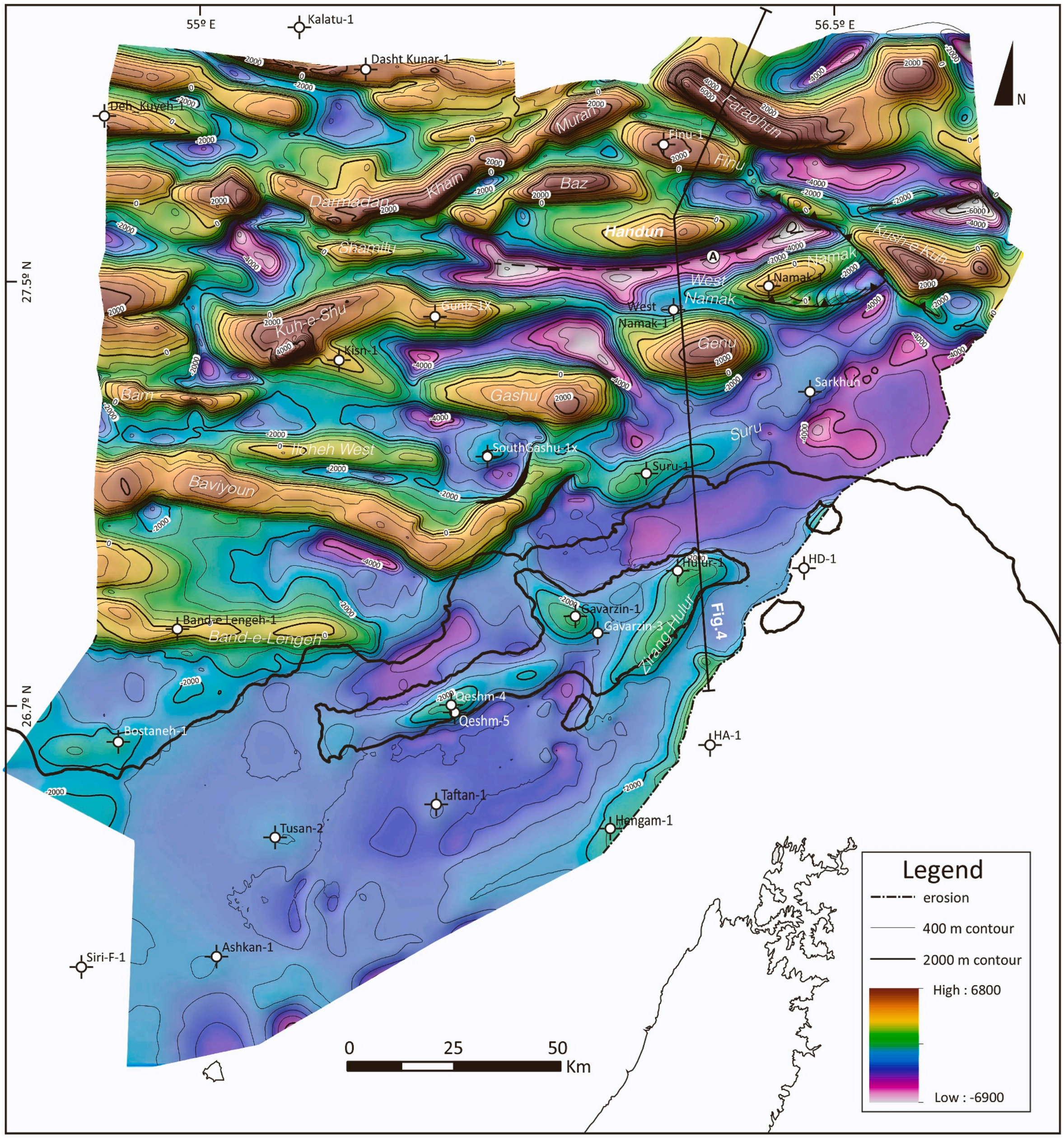

Fig. 5. Complete 3D model of the top of the AsmariFm. in the Eastern Fars region. Additionally, the main anticlines, the placement of wells employed for the 3D reconstruction and the regional cross section are indicated. The letter A highlights the south-dipping basement normal fault interpreted at depth.

Upper Cretaceous to Miocene units away from the crest is likely due to the folding and rejuvenation of the underlying salt structure.

To the north of the Suru anticline, the Kalat Bala structure is interpreted as a passive diapir formed from Hormuz Salt, with its development spanning from the Paleozoic to the Miocene and underwent squeezing during contraction. However, the more recent Cenozoic units exhibit minor folding and limited deformation, implying that this structure experienced relatively less impact from the Zagros contractional event compared to other salt structures in the vicinity. Unlike most salt structures in the area, the Kalat Bala structure is positioned along a syncline axis, rather than functioning as a salt body that triggers the initiation of folds or thrusts, similar to those mentioned earlier. Analog models (e.g., Santolaria et al., 2020) propose that a significantly disharmonic location concerning the spacing pattern of folds and thrusts facilitates the passive displacement of nearly undeformed salt bodies within contractional settings.

Moving further north, the Genu structure forms an anticline spanning approximately 25 km wide. Its significantly larger wavelength compared to other structures indicates the presence of a thicker stratigraphic sequence detached from the underlying basement, rather than a thinner sequence folded over an inflated salt body. The anticline's position also coincides with the inflection point where the regional flexure transitions from a southward dip to a northward dip. On its northern limb, a narrower fold known as the West Namak anticline emerges as the Genu structure deepens toward the north, reaching its lowest structural elevation about 5 km south of the Handun anticline. In the syncline hinge, the base of the Miocene sequence lies at a minimum depth of approximately 4 km (Fig. 4e), which is 2 km deeper than in the southern and northern synclines. The significance of this regional structural offset can be associated with salt evacuation or a basement structure, which will be discussed further in chapter 7.1.

The Handun anticline exhibits a prominent asymmetry, with a gently dipping northern limb and a nearly vertical southern limb, cut by a north-dipping blind thrust at depth. The interpreted fault is seismically active, with several recorded events (e.g., the 2021 M_w 6.2 shock) and associated surface deformation, suggesting a thrust fault plane located at depths ranging from 7 to 9 km, affecting the sedimentary cover and uplifting the hanging-wall.

North of the Handun anticline, the base of the synclines shows a progressive 2° steepening of the regional detachment until the Faraghun structure, where the Paleozoic succession thrusts over the Mesozoic and Cenozoic deposits. In map view (Fig. 1), this fault contact exhibits significant changes in geometry: it is a back-thrust to the SE and an almost vertical contact toward the NW, where the cross-section passes through. Here, this contact delimits the northern and southern limbs of the Faraghun Anticline, and is characterized by the presence of several patches of Hormuz Salt. To the south of this contact, the Mesozoic and Paleozoic sequence is missing, suggesting the presence of a former diapir which was squeezed and subsequently secondary welded during the contraction. This anticline presents also significant thickness variations between the two limbs, at the footwall and hanging-wall of the thrust respectively (Fig. 4). The Jurassic and Lower Cretaceous sediments are thicker in the southern limb, whereas the Sarvak, Gurpi, Pabdeh and Jahrum Fms. are thicker in the northern limb.

These thickness variations are attributed to differential subsidence during the Triassic extensional event, which effects reached the Jurassic and Lower Cretaceous sequences until the entire succession was welded. Subsequently, coinciding with the onset of the contractional setting, the northern limb subsided in the Zagros orogen foreland (Fig. 4).

A palinspastic restoration of the regional cross-section up to the top of the Oligocene (Fig. 4a) was undertaken. For this restoration, a pin line located 20 km south of the Zirang-Hulur structure was used, as deformation southwards of this line was deemed negligible. Shortening calculations were performed for the aforementioned geometries. These geometries were reconstructed above the topography using the geometric approach that involves minimum shortening (Fig. 4b).

The process of cross-section balancing enabled us to estimate a total shortening of 19 km, representing for 12% of the total length of the cross-section. This shortening estimate covers the period from the Miocene to the present and is comparable, falling within the same range as the recently published N-S section by Hinsch et al. (2022), located approximately 80 km to the west, with a value of 14.7%.

5. Top Asmari 3D model

This reconstructed 3D elevation model (Fig. 5) corresponds with the spatial distribution of the upper Chattian units. It represents the top of the Asmari Fm. within the onshore region, extending offshore to the top of the Pabdeh Fm. In the northeastern sector, where the transition from Asmari to Razak Fms. occurs gradually, the model delineates the base of the Razak Fm.

The 3D model vividly illustrates the geometry of the pre-folding succession, considering that the basal boundary of the syn-folding deposit dates to the Miocene. This allows a better picture of the structural offsets for both synclines and anticlines. The reconstructed surface ranges from 6800 m above to −6900 m below sea level and is truncated by erosion in the south-eastern sector of the study area (Fig. 5). Anticline trends range from broadly E-W, consistently with structural grain west of the study area, to NE-SW trend (e.g., in the Shu or Darmadan-Khain-Muran) and to NW-SE, as shown in the Gahkum, Faraghun, and Kush-e Kuh in the proximities of the High Zagros fault (Fig. 1). In a similar fashion to other salt-detached contractional systems, the structural taper angle is ~1.5°, and structures generally lack a dominant structural vergence. Superimposed on this low regional taper, there are prominent structural offsets, especially in the more central zones of the study area. Structural highs (ca. 6000 m high) include the Shu NE-SW-trending anticline, or the Faraghun structure. A remarkable E-W-trending structural low emerges from the east (labelled with “A” in Fig. 4), passing through the Kush-e Kuh anticline and forming a distinctive saddle-shaped geometry within the structure. Continuing as a syncline to the south of the Handun anticline, it then extends westward, potentially influencing the structural elevation of the Shamilu Anticline. Along this trough the highest depths of the Asmari Fm. are found, reaching their deepest points within synclines that are located at depths of around −5000 m and occasionally exceeding −6000 m (north of Khush-e Kuh anticline and east of Handun anticline).

6. The Handun diapir

The Handun anticline, extending 40 km in an east-west direction, is characterized by a double-plunging geometry and spans around 7 km in width at its surface. It is cored by the Hormuz Salt which crops out in the central part of the structure (Fig. 3) and represents the surface expression of the Handun diapir. The sequence cropping out in the Handun anticline includes the Precambrian Hormuz Salt, the Eocene to Oligocene Jahrum Fm., the Miocene Razak and Mishan Fms. (as well as the Guri Mb.), the Miocene to Pliocene Aghajari Fm. and the Pliocene to Pleistocene Bakhtiari Fm., which is preserved in the core of the structure directly of top of the Hormuz Salt (Fig. 3)

At the surface, the Handun anticline displays an almost symmetrical configuration, characterized by dips of 40° to 45° in both of its limbs. Nonetheless, a convergence of the anticline flanks become evident in the region where the Hormuz Salt crops out, leading to a narrowing of the structure and dividing it into two distinct sectors. The eastern part of the anticline, is narrower than the western one and presents a plunge of around 12° to the east except in the vicinity of the diapir where the plunge shifts 14° to the west (Fig. 3). On the other hand, the wider western part exhibits a plunge of 4° to the west except near the diapir where it sharply shifts to an eastward plunge of 4.5° (Fig. 3). Remarkably, a distinctive network of radial normal faults is present in close proximity to the diapir. These faults exhibit offsets ranging from decametric to hectometric scales, affecting the Jahrum Fm. through to the Mishan Fm. (Fig. 3).

High quality halokinetic sequences are prominently exposed around the Handun diapir, providing insights into the interplay between sedimentation of the overburden strata and salt raise over an extended temporal and spatial scale (Figs. 6 and 7). This remarkable preservation allows for the observation of the diapir evolution from the Paleocene to the Pliocene, describing the distribution of facies and the salt-related geometries within each unit exposed around the Hormuz diapir. The oldest of these unit exposed is the Paleocene to Eocene Jahrum Fm. This formation is characterized by organodetrital carbonates rich in Nummulites, along with shoal deposits of coarser shell material, that indicate deposition in higher energy paleoenvironments. Additionally, dolomitization and chalkiness are commonly observed near the top of the formation. In close contact with the diapir, the Jahrum Fm. consists of conglomerates and sandstones (Fig. 8a). These facies are part of the halokinetic sequences (Faridi et al., 2021; this study) and exhibit a sudden disappearance as one moves away from the influence of the diapir. Near diapir basal deposits above the halokinetic sequence boundaries comprise carbonate debris-flow facies that contain clasts in a silty to sandy carbonate matrix. Debris-flow clasts were mainly derived from non evaporite lithologies present within the Hormuz Fm. (Fig. 7).

In the vicinity of the diapir, the earliest layers of the Jahrum Fm. exhibit folded geometries spanning several meters. These folded sequences often involve overturned strata and are overlaid and truncated by a similar folded sequence (Figs. 9 and 10 and, 11a).

These particular geometries are known as “hooks” and are considered halokinetic structures resulting from drape folding (Rowan et al., 2003). These hooks develop as sediments around the Handun diapir subsided simultaneously with the upward movement of the underlying salt (Giles and Rowan, 2012). The tabular halokinetic sequences associated with these hooks are further characterized by remaining patches of extruded salt that controlled the folding, forming what are commonly referred to as "cusps" (Rowan et al., 2020), which are exposed at the diapir’s edge (Fig. 11a).

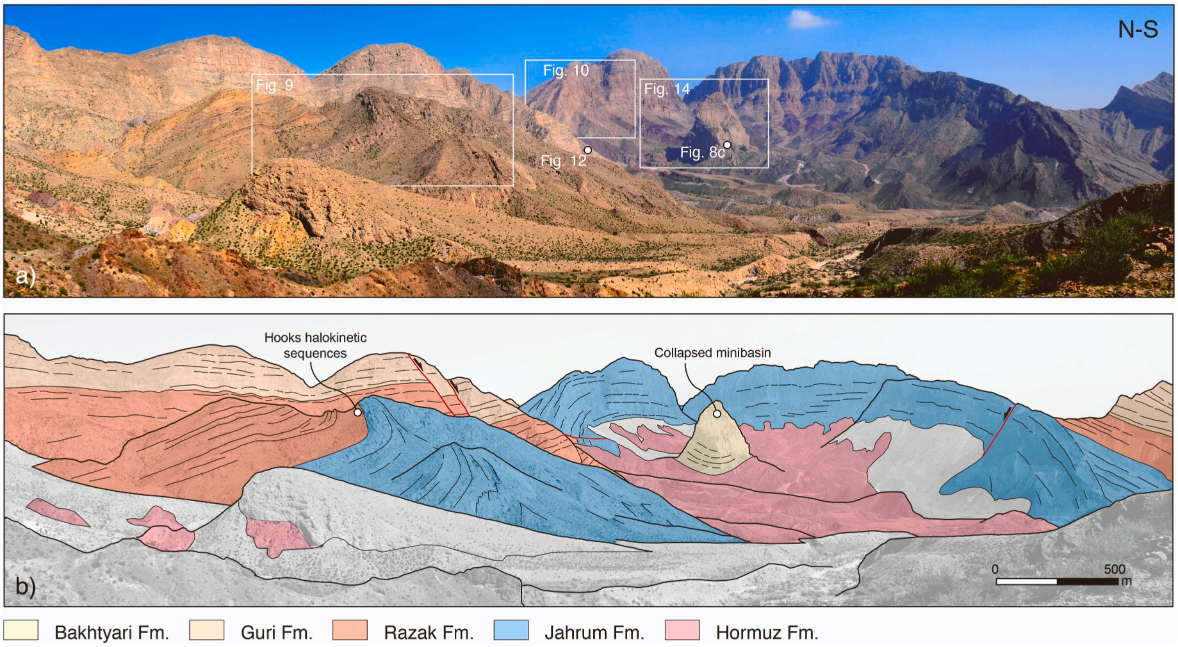

Fig. 6. E-looking panoramic view of the Handun anticline. a) Uninterpreted photography. b) Line-drawing and main units and structures. See Fig. 3 for location.

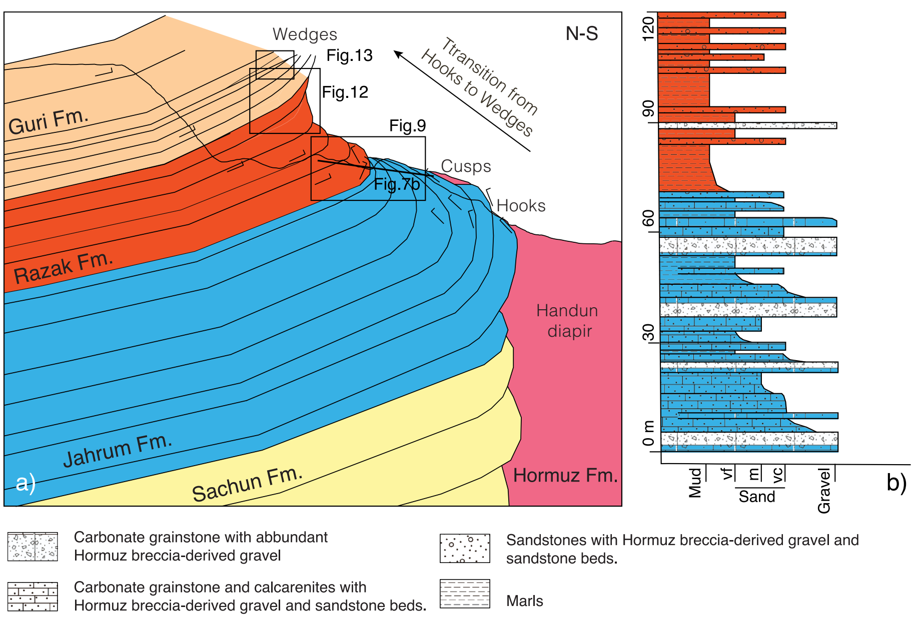

Fig. 7. a) N-S Schematic cross-section of the halokinetic sequences within the Handun anticline (refer to Fig. 3 for location). b) Detailed field stratigraphic log through the various hooks in the Jahrum and Razak Fms. The base of each halokinetic sequence indicates a fining-upward sequence with basal deposits containing abundant clasts sourced from the Hormuz diapir.

Faridi et al. (2021) have provided alternative interpretations of these relationships, suggesting episodes of extrusion and emplacement of the Hormuz Salt-sheets within the Jahrum Fm. While they present interpretations illustrated on draped satellite images (Figs. 6 and 7 in Faridi et al. (2021), our field-based experience suggests that in the Hormuz Salt is not emplaced in the specified stratigraphic interval but just present as patches of the eroded edge of the diapir or strictly related to the drape folds.

In contrast, on the western edge of the diapir, halokinetic sequences that emerge within the Jahrum Fm. display wedge-like geometries within the sedimentary package (Fig. 11b, c and d). Notably, there is a transition in dips from vertical to gently dipping over a span of tens of meters moving away from the diapir. These wedges incorporate distinctive features, including onlaps, bed thickening, and low-angle truncations (<10°), which stand in contrast to the tightly folded configurations observed in the hooks situated farther to the east (Fig. 11a).

The Jahrum Fm. is overlain by the Oligocene to Miocene Razak Fm., made up by silty sandy marls and red beds. Within this formation, there are hook sequences that range in thickness from decametric to hectometric scales (up to a maximum of 200 m) (Figs. 9, 10 and 12), and related facies changes with abundant debris deposits derived from the Hormuz Salt (Fig. 8b).

The upper segment of the Razak sequence displays tabular halokinetic sequences that gradually transition into growth strata formed

Fig. 8. a) Hormuz and Jahrum clasts within the Jahrum Fm. b) Detailed photo of the Razak Fm. in close contact with the Handun diapir (see Figs. 6 and 14 for location). In this area Razak Fm. is made up of conglomerates and sandstones mainly formed by components derived from the erosion of the Hormuz Salt. These coarse-grained facies disappear away from the diapir. c) Detailed photo of the recent deposit preserved in the core of the Handun diapir with clasts mainly by Hormuz exotic material and Guri Limestones. A 28 cm long geological hammer, an 8 cm high GPS unit, and a 14 cm pencil are included for scale.

by wedges (Fig. 12). The boundary with the overlying Middle Miocene Guri Mb. is found to be conformable. This Guri Mb. also encompasses halokinetic sequences characterized by wedge geometries, arranged in composite sequences that exhibit tapering patterns (Figs. 13 and 7).

Overlying the Guri Mb. is the Middle to Late Miocene Mishan Fm., which primarily consists of shallow-water marine marls interbedded with bioclastic layers. Unfortunately, the contact between this unit and the Hormuz Salt is not preserved.

In the central part of the structure, a substantial pile of conglomerates, several hundred meters in thickness, crops out. These conglomerates which, unconformably overlie the Hormuz Salt, are folded into an open syncline (Figs. 3 and 14). They are made of massive and thick-bedded, coarsening upwards fluvial deposits, consisting of polymictic conglomerates with numerous clasts of Hormuz Salt and cross-bedded sandstones. In terms of facies, these conglomerates and sandstones

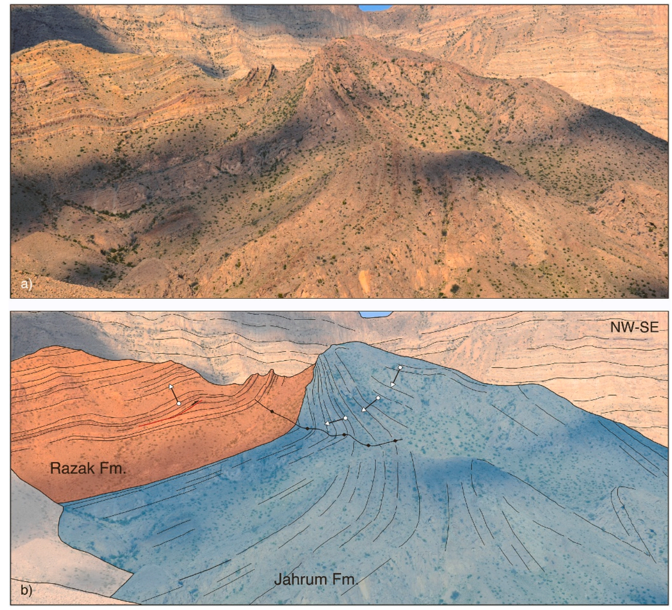

Fig. 9. Halokinetic sequences and related hooks cropping out within the Handun anticline in the Jahrum and Razak Fms. (see Figs. 3 and 6 for location). (a) shows the original, uninterpreted photograph, while (b) provides a line drawing and interpretation of the same view. The outcrop shows how the beds are folded near the diapir, but they recover the regional dip in a short distance. Notice the thickening of units downwards.

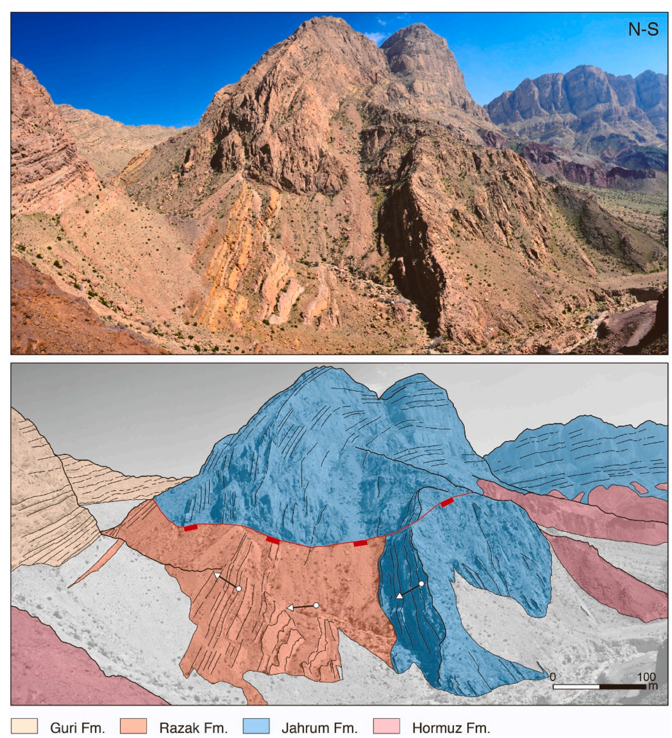

Fig. 10. Field view of one of the radial normal faults in the Handun anticline (see Figs. 3 and 6 for location). The fault is N-S oriented and dipping westward. In the hanging-wall of the normal fault, over 400m of Razak and Jahrum succession, progressively change from a 45° north-dipping normal flank to an overturned flank dipping about 30° to the south, describing a Hook geometry in contact with the Hormuz Salt.

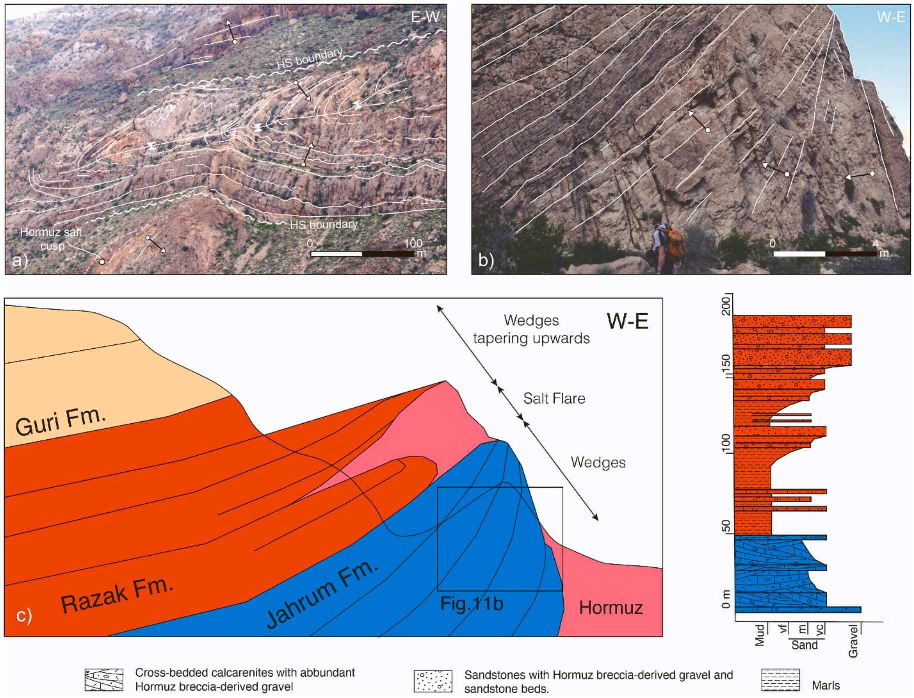

Fig. 11. Interpreted detailed photographs of Jahrum outcrops in close contact with the Handun diapir (see Fig. 3 for locations). a) Example of the geometries observed in the southern flank of the Handun anticline. In the main structure at the center of the image, beds are folded into an overturned limb and form a hook halokinetic sequence, bounded upwards by a sharp truncation. The hook underneath shows itself an overturned and truncated flank, overlain by an outcropping patch of Hormuz Salt. b) Geometries observed in the western edge of the diapir are characterized by wedges and a sequence of progressive angular unconformities. c) W-E Schematic cross-section of the halokinetic sequences within the Handun anticline (refer to Fig. 3 for location). d) Detailed field stratigraphic log through the halokinetic sequences in the Jahrum and Razak Fms.

bear resemblance to those found within the Bakhtiari Fm. (Fig. 8c). However, it's important to highlight that the youngest identified clasts within these units are pebbles originating from the Guri Mb.

This suggests the possibility that these conglomerates and sandstones are also potentially age-equivalent to either the Mishan or Aghajari Fm. Regardless, based on the age assignment of these conglomerates, it is evident that they are located a minimum of 1.5 km below their corresponding structural level.

7. Discussion

7.1. The role of basement inheritances

The balanced cross-section presented in this work (Fig. 4) reinforces the structural style found in other salt-detached fold and thrust belts, i. e., low taper angle, no dominant structural vergence, and a wider section with respect to non-salt-involved equivalents (Davis and Engelder, 1985). However, the basal level of the interpreted synclines (Figs. 4 and 5) underscores the presence of substantial structural offsets. At the regional scale, the broader flexural response within the Zagros and Oman chains accounts for up to 3 km of lithospheric tilting. On a more local scale, structural offsets (e.g., as the one observed in Handun frontal limb) can be attributed to three factors. i) thrusting and disharmonic folding in a thin-skinned scenario ii) the role of basement-involved faulting, and, iii) changes in the stratigraphic thicknesses.

The presence of significant imbrications can be ruled out given the low taper angle observed in the study area, as also demonstrated in several analog modelling studies (Ruh et al., 2012; Nabavi et al., 2023).

However, determining the extent of basement involvement, whether major or minor, poses a challenge. The uncertainties in constraining a suitable interpretation at depth are primarily related to the knowledge of the stratigraphic thickness and depend on the quality and selection of the used sources. Depending on the choice of data, whether it be derived from outcrop observations, geological mapping, or subsurface sources like well data and seismic reflection profiles and the related time to depth conversion procedures, the accuracy and reliability of the interpretation can vary significantly.

Additionally, the thickness of the stratigraphic template is significantly influenced by both the variation in dip of the detachment level or top basement, as well as by halokinetic or tectonic processes and their chronological sequencing (Butler et al., 2018). Recognizing the significance of these parameters in the results of section balancing is of paramount importance (Hinsch et al., 2022). However, the relatively limited constraints on these factors in the Eastern Fars region have led to divergent interpretations concerning the extent to which the basement-involved faults played a role beneath the Hormuz Salt layer in the deformation process.

Several previous solutions have been proposed, including thin- and thick-skinned solutions for the same section. In the former scenario, positive changes in the structural elevation have been addressed to partial welding or differential subsidence, resulting in remanent areas of inflated salt plateaus (e.g. Jahani et al., 2009; Callot et al., 2012.). In the latter scenario, most of the published interpretations consider active contribution of basement thrusting (e.g., Molinaro et al., 2005; Letурmy and Robin, 2010; Tavakoli et al., 2013).

However, the presence of significant structural offsets that affect the regional elevation which could potentially be related to thick-skinned tectonic processes as observed in other regions of the Zagros, remains less distinct in eastern Fars. Seismological evidence is not conclusive, and recent studies relocated the focal depth estimates to shallower levels, suggesting that most large earthquakes in the Zagros are contained within the mid-lower sedimentary cover and that the crystalline basement shortens mostly aseismically (Nissen et al., 2011, 2014).

Northwest of the Fars region, a more precise interpretation is given to the frontal positive structural offset referred as the Mountain Front Flexure located along the external Zagros. This structure is considered a

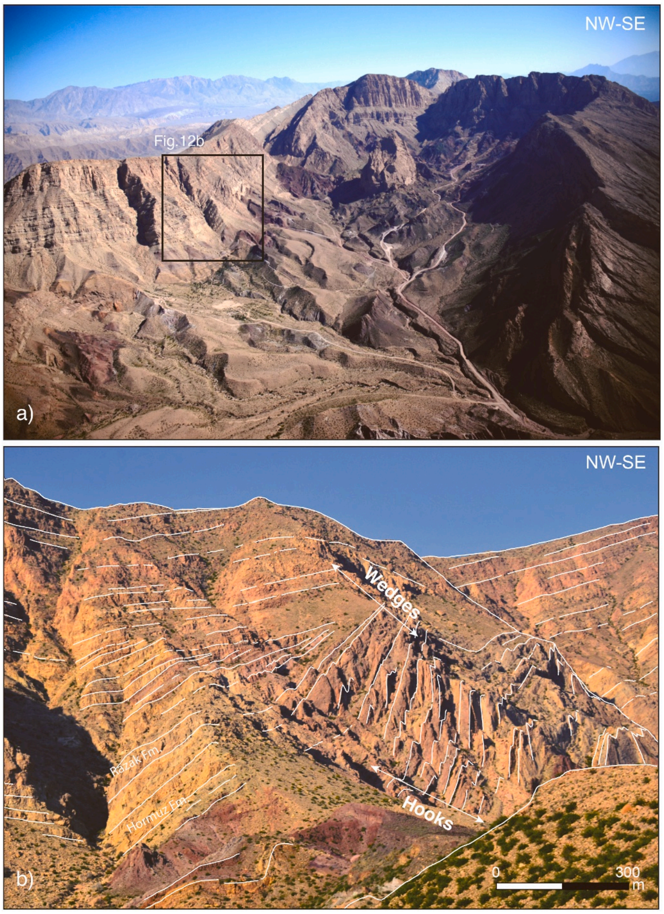

Fig. 12. Northward view of the Handun anticline, taken from a helicopter. The Razak halokinetic sequence are spectacularly exposed on the northern flank, with Fig. 12b providing a closer view. b) View on the northern flank of the Handun anticline (see Figs. 12a, 3 and 6 for location). The Razak Fm. is in contact with the Hormuz Salt in the lower valley and shows vertical to slightly overturned dips. The upper part of the Razak sequence loose dip by progressive angular unconformity, forming wedge geometries. Above, the Razak Fm. is overlayed and truncated by the Guri Mb.

Fig. 13. Image of the Guri Mb. in the northern limb of the Handun anticline (see Figs. 3 and 6 for location). Here the geometry of the halokinetic sequence is characterized by wedges defining stacked tapered sequences. As a consequence, the rate of salt rise vs sedimentation decreased with respect to the Jahrum and the lower Razak Fms.

major element of the Zagros orogenic system and is intrinsically linked with the underlain deeply rooted and seismically active Mountain Front Fault system beneath it. The role of the Mountain Front Flexure has been comprehensively investigated, and data suggest an hybrid tectonic style characterized by a major and newly developed crustal ramp in the frontal portion of the belt (i.e., the Mountain Front Fault) and by the reactivation of steeply dipping pre-existing basin-bounding faults, along with a minor amount of shortening in the inner area (Tavani et al., 2020).

However, the reconstructed 3D elevation model (Fig. 5) stresses that positive structural offsets in the Eastern Fars lack in lateral continuity compared with the mentioned Mountain Front Flexure, besides they are present just along few structures in the inner areas of the folded belt, as the NE-SW-trending Shu, or the NW-SE-trending Khush-e-Kuh and Faraghun anticlines.

Differently, the E-W-trending structural low located south of the Handun anticline is a prominent feature that extends for over 150 km affecting several structures of the Zagros fold and thrust belt structural grain. East of Khush-e-Kuh, at the junction between the N-S-trending Zendan fault and the eastern limit of the Makran accretionary prims, the 3D elevation model reaches ~ -6800 m (b.s.l.). At this location, a sharp transition occurs, featuring a structural offset of more than 2 km to the north, pointing to the presence of a south-dipping normal fault affecting the pre-Miocene sequence. Moreover, in the same structural position, both offshore and onshore, there are indications of similar extensional faults that were active during the Upper Cretaceous to Oligocene period, coinciding with the local development of foreland basins along the Arabian margin (Orang et al., 2017).

Moving westward, the Khush-e-Kuh anticline exhibits a noticeable increase in structural plunge crossing the E-W structural low, forming a saddle-like geometry. These observations lend support to the hypothesis of the presence of inherited basement-involved normal faults that could affect the depth of the detachment. Given the resemblance with other internal sectors of the Zagros, such as the mentioned Lurestan arc and Kirkuk embayment, it is plausible to posit the existence of a pre-existing rift architecture in the Fars region. However, our suggestion is that the presence of an effective basal detachment, such as the Hormuz Salt, has hindered the inversion, especially for the more proximal extensional system. Instead, the deformation has been translating the deformation to the more external structural units.

Accordingly, we interpret that the Handun diapir formed on a basement structural high (Peacock et al., 2020) inherited from previous rifting. During the shortening, the Handun anticline was detached and its southern limb transported southwards above the hanging-wall of a basement south-dipping normal fault. As a consequence, and probably promoted by the contraction (Humphris, 1978, 1979; Rowan et al., 2002), the forming south growth syncline subsided into over 2 km thick Hormuz Salt, while the back limb remained in the footwall, i.e., in the structural high.

To sum up, our restoration yields a total of 12% of shortening, entirely accommodated by detachment folds in a thin-skinned setting.

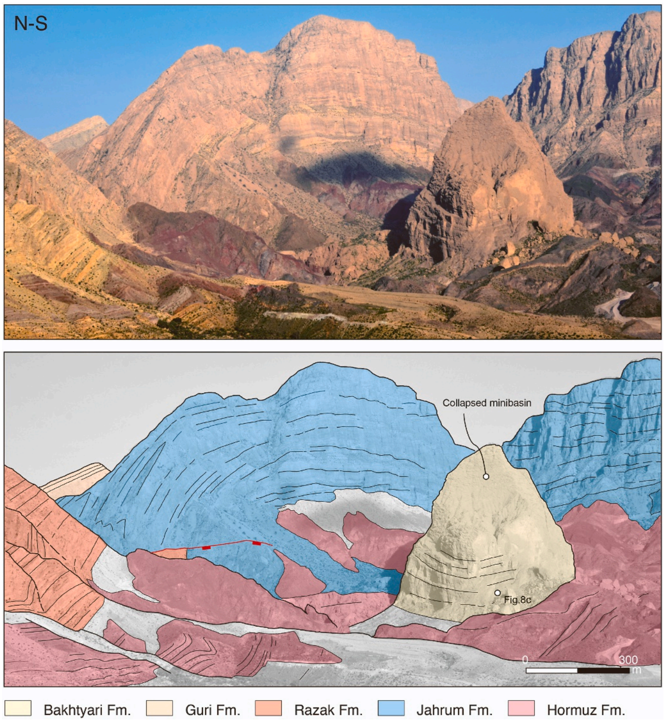

Fig. 14. E-looking panoramic view of the Handun anticline, (see Figs. 3 and 6 for location). Conglomerates of the Bakhtiari Fm. crop-out at the center of the diapir. Notice the open syncline deforming the conglomerates unconformably overlaying the Hormuz Salt. The presence of these conglomerates implies that the upper part of the crest subsided into the diapir stem as a consequence of a decreese in the salt rise rate, probably related to the development of a secondary weld.

Such detachment folds laid above a pre-existing faulted basement framework. Indeed, the calculated displacement of 9 km to the south of its pre-contractional position, as proposed by Hinsch et al. (2022), falls well within the suggested range. This finding strongly indicates that the initial triggering of diapirism occurred above the shoulder of a basement normal fault during the early Paleozoic era, predating any subsequent contractional event (Fig. 14a).

7.2. The Handun diapir evolution

In this section, we untangle the role of different key elements that control the main deformative stages of the Handun diapirism. Our focus spans from its initial triggering, the subsequent passive growth, the rejuvenation of the diapir and the timing of primary and secondary welding processes. Finally, we propose a sequential restoration for each evolutionary step (Fig. 15).

In the preceding chapter, we introduced a structural framework outlining the pre-shortening configuration of the Handun diapir (Fig. 15a). Nonetheless, our understanding of the Paleozoic and Mesozoic evolution of the Handun diapir remains limited due to the absence of direct observations. The tectonic history of the eastern Arabian Margin during the purported Paleozoic “Hercinian” stage remains enigmatic, and our understanding of the Neotethyan Permo-Triassic to Jurassic extensions is constrained by limited evidence. Several prior studies suggest an early triggering of diapirism, occurring during early Paleozoic, soon after the late deposition of the Hormuz Salt sequence and followed by a prolonged stage of passive growth (Jahani et al., 2009; Perotti et al., 2016; Snidero et al., 2020).

A different interpretation is depicted by other authors (Fig. 10 in Faridi et al., 2021), where the Paleozoic passive stage of the Handun diapir is preceded by the deposition of a significant Paleozoic

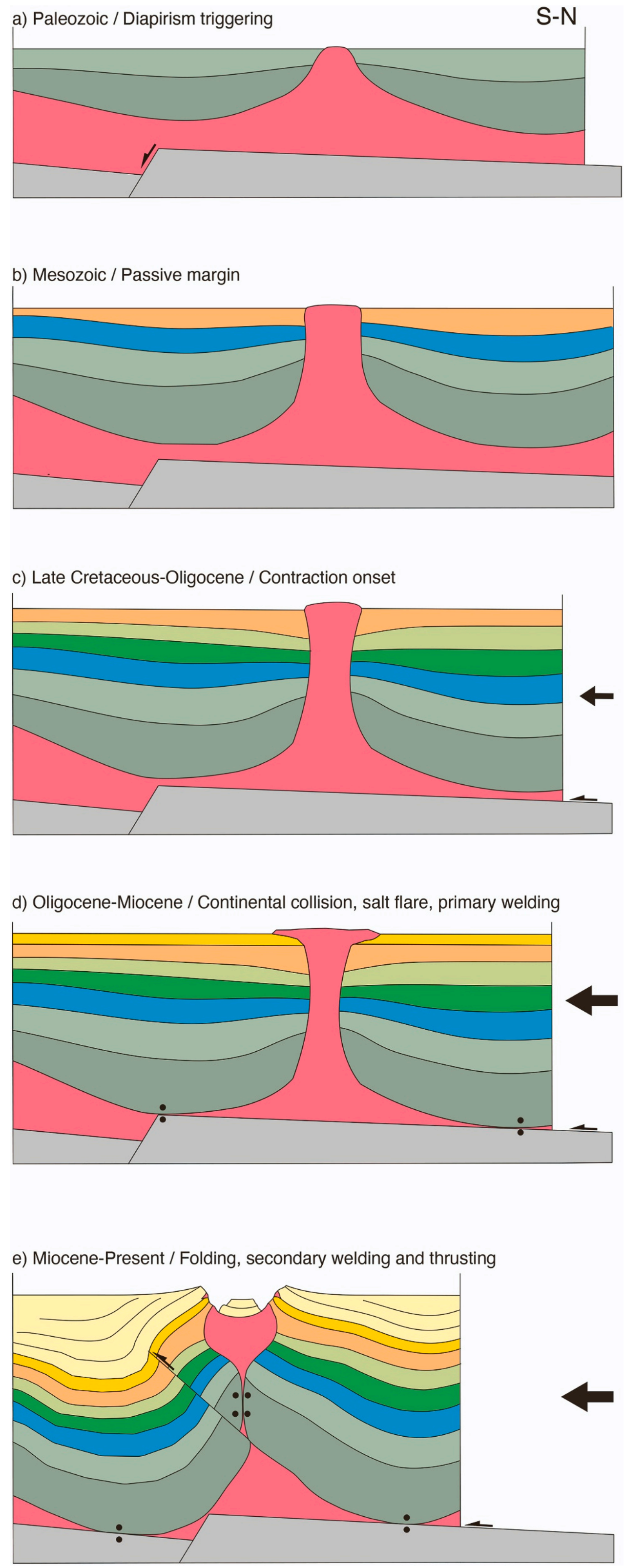

Fig. 15. Sequential restoration of the Handun structure. a) Triggering of the salt structure and passive growth by sedimentary loading. b) Passive growth of the diapir during most of the Mesozoic, in a passive margin setting. c) Onset of the contractional deformation and growth of the diapir. d) Rejuvenation of the diapir synchronous with the continental collision, leading to the flaring and lateral expansion of the Hormuz Salt. e) Squeezing of the diapir during the continuate contraction and folding until the formation of a secondary weld and causing a secondary minibasin to subside.

overburden, eventually pierced in a subsequent stage. While we acknowledge their perspective, we believe that explaining a truncation relationship between the Hormuz Salt and the Paleozoic sequence would be unlikely (Vendeville et al., 1991), particularly considering the absence of documented instances of megaflaps.

During the Neo-Tethyan rifting, the extension might have had an impact on diapirism, potentially even reactivating its growth if early burial occurred. However, the only available data on extensional structures in the overburden are of poor quality and located over 400 km away in the Dezful Embayment (Sepehr and Cosgrove, 2004).

So, even though rifting significantly affected the basement in the Fars region, the degree of decoupling between the basement and the cover remains unclear.

Instances of Jurassic and Cretaceous halokinetic sequences have been documented in analogous structures within the region (e.g., the Darmadan diapir, Snidero et al., 2019 or the Tunb diapir, Snidero et al., 2020), suggesting an ongoing passive growth of the diapirs throughout the Mesozoic (Fig. 15c). The possibility of a significant burial (e.g., over 1 km of overburden) should also be excluded considering that piercement of such cover without any significant thinning is impossible (e.g., Jackson et al., 1994). Furthermore, there is no evidence of major flaps from either field observations or seismic data. This leads to the conclusion, that Mesozoic, pre-contractional salt structures in Fars mainly consist of passive diapirs (Fig. 15c), as suggested by previous authors (e.g. Callot et al., 2012; Perotti et al., 2016; Motiei, 1995).

Conversely to the uncertainties when reconstructing the Mesozoic diapir evolution, the Cenozoic deformation history is well-constrained by the presented field work and the direct observations of the stratigraphic and structural relationships between the Hormuz Salt and its stratigraphic overburden. From Late Cretaceous and responding to the onset of contraction, Hormuz diapirs were rejuvenated. The presence of hook halokinetic sequences in the Jahrum and Razak Fms., along with the occurrence of clasts sourced from the Hormuz Salt, provides clear evidence that the Handun diapir raised and reached the surface throughout the Paleocene to Middle Miocene times. These observations imply a state of diapir growth, characterized by similar rate of salt rise compared to the sedimentary accumulation rate. This interpretation is further supported by the stacking of tabular composite halokinetic sequences (Fig. 15c).

Beyond this general characterization, what is interesting is that the observed halokinetic sequences also exhibit lateral changes, transitioning from hooks in the central part of the diapir to wedges in its western termination. This suggest a highest salt flow in the center of the diapir which is consistent with its peanut geometry (Fig. 3).

In the upper section of the Jahrum sequence, laterally equivalent to the Eocene to Oligocene Asmari Fm. the ongoing growth of the diapir, transitions to more intense activity. This diapir rejuvenation occurs as a synchronous response to the onset of continental collision.

The Hormuz Salt advances through the stratigraphic sequence above the strongly overturned composite halokinetic sequence, suggesting the flaring of the diapir and the expansion of the salt's influence into Razak deposits located at more distance from the diapir feeder (Fig. 11c and d).

The continued extrusion and flaring of Hormuz salt, especially affects the lower sequence of the Razak Fm., leading to the formation of well-developed hook halokinetic sequences, and the deposition of detrital material sourced from the Handun diapir (Figs. 10, 11c and 11d and 12).

The peak of the episodic extrusion is marked by several Hormuz Salt patches cropping out around the Handun diapir, emplaced at the top of the lower approximately 100 m thick, marly sequence of the Razak Fm. (Figs. 1, 3 and 15d).

Interestingly, regional contraction has affected the more internal structures of the Zagros Mountains since the Late Cretaceous, as seen in structures like the Darmadan diapir, which experienced early squeezing and a similar flaring of the Handun diapir, during the initial stages of contractional deformation, coinciding with the transition from obduction to continental collision along the northeastern edge of the Arabian plate (Snidero et al., 2019).

Within the upper portions of the Razak Fm., despite the expected increase of salt rise by squeezing and rejuvenation of the former passive diapir, a clear transition from tabular composite halokinetic sequences to tapered ones is observed. This transition points towards a relative reduction in the rate of salt rise compared to the sedimentation rate, implying a decrease of the salt input because the stem is nearly secondary welded and/or the mother source layer almost depleted or disconnected from the stem by primary welding (Fig. 15e). Subsequent active rise of the diapir could also explain the generation of the observed radial faults in the aggrading overburden. Shouldering-aside and burial of the roof along the flanks may expose these strata to stem push–related stresses, re-activating preexisting, or forming new, radial faults (Nikolinakou et al., 2014; Coleman et al., 2018).

The final stages of the diapir's evolution are deduced from the conglomerates exposed within the central region of the diapir. The distribution of these conglomerates, combined with the evident configuration of an open syncline, suggests that they are filling a small secondary minibasin subsiding in the stem of the diapir. Consequently, it is plausible to infer the presence of a secondary weld at depth, facilitating the eventual collapse of the upper portion of the diapir (Fig. 15e). Although the exact age of these conglomerates remains uncertain, they clearly post-date the interpreted Miocene primary welding.

8. Conclusions

This study aimed to unravel the tectonic evolution of the Handun diapir within the broader context of the Zagros fold and thrust belt. Through comprehensive fieldwork, analysis of structural elements and analog comparisons, we have described the formation, growth, and deformation history of the diapir.

By employing cross-section balancing techniques, we have successfully estimated a total shortening of 12% accommodated by thin-skinned deformation. Although interpretations differ regarding the role of the basement-involved faults, evidence suggests the existence of structural offsets related to thick-skinned tectonic processes. The Handun diapir formed on an inherited basement structural high inherited from previous rifting and was subsequently detached and transported above the hanging-wall of a basement extensional fault, leading to subsidence into over 2 km of the Hormuz Salt. Our interpretation suggests that the effective basal detachment created by the Hormuz Salt played a crucial role in hindering inversion and redirecting the deformation towards the external structural units.

The Handun diapir experienced prolonged phases of growth throughout the Mesozoic and Cenozoic. The potential for diapir rejuvenation is explored, specifically during the sedimentation of the Oligocene-Miocene Jahrum, Razak and Guri Fms. Our findings highlight the temporal and spatial variability of salt rise rates.

The squeezing of the passive diapir is revealed by the halokinetic sequences in the Jahrum sediments and the along strike transition from wedges to hooks toward the central part of the salt wall, where a peanut structure developed. During the deposition of the upper Oligocene-lower Miocene Razak Fm., continuous shortening increased the salt flow rate relative to the sedimentation rate, leading to the flaring of the diapir and the development of hook halokinetic sequences. Later, halokinetic sequences transitioned to wedges during the deposition of the Guri Fm., indicating a slowdown in salt flow, either by primary welding or by narrowing of the diapir stem before secondary welding. Evidence of secondary welding, as contractional deformation progressed, is shown by the collapse of the upper part of the diapir and the formation of a secondary minibasin.

Overall, the structural evolution of the Handun diapir, as revealed by field observations and constrained by regional cross-section construction, provides further insights into the evolution of salt structures in the Fars area of Zagros and diapirs in general.

CRediT authorship contribution statement

Marco Snidero: Writing – review & editing, Writing – original draft, Visualization, Validation, Supervision, Methodology, Investigation, Formal analysis, Data curation, Conceptualization. **Josep Anton Muñoz:** Project administration, Investigation, Funding acquisition, Conceptualization. **Pablo Santolaria:** Writing – review & editing, Investigation. **Nuria Carrera:** Investigation, Data curation. **Mireia Butille:** Investigation, Formal analysis, Data curation.

Declaration of competing interest

The authors declare that they have no known competing financial interests or personal relationships that could have appeared to influence the work reported in this paper.

Acknowledgments

We acknowledge the support of the research project Structure and Deformation of Salt-bearing Rifted Margins (SABREM), PID2020-117598 GB-I00, funded by MCIN/AEI/10.13039/501100011033, and the VIG-EOOCULT (PLEC2021-007903) and GEODIGIT (TED2021-130602B-I00) research projects funded by MCIN/AEI/10.13039/501100011033 and for the European Union “NextGenerationEU”/PRTR. The GEOMODELS Research Institute and the Grup de Geodinamica i Analisi de Conques (2021SGR76) are also acknowledged for their financial support. We gratefully acknowledge the National Iranian Oil Company for providing the subsurface data. We would like to express our gratitude to Ali Faghih for handling the review process of this article and to the two anonymous reviewers, whose contributions went far beyond the standard peer-review process. Schlumberger® is thanked for providing the Petrel E&P software for subsurface data interpretation. Special thanks are directed towards SKUA-GOCAD® software and Midland Valley® 3D Move for providing the indispensable tools used in constructing the structural model, cross-section and the surface reconstruction processes.

Data availability

Detailed list of recorded structural data, utilized for constructing the 3D model and the cross-section, are accessible in an open-access repository (Snidero, 2023).

References

Adineh, S., Zavada, P., Bruthans, Cofrade G., Zare, M., 2024. Growth of a salt diapir in an anticline - a record from the Cenozoic halokinetic sequences in the Zagros Fold and Thrust Belt, Iran. J. Struct. Geol. 178, 105004. https://doi.org/10.1016/j.jsg.2023.105004, 2024.

Alavi, M., 2004. Regional stratigraphy of the Zagros Fold-thrust belt of Iran and its proforeland evolution. Am. J. Sci. 304, 1–20.

Alavi, M., 2007. Structures of the Zagros Fold-thrust belt in Iran. Am. J. Sci. 307, 1064–1095. https://doi.org/10.2475/09.2007.02.

Alsouki, M., Ali, Riahi M., Yassaghi, A., 2011. Seismic imaging of sub-circular salt-related structures: evidence for passive diapirism in the Straits of Hormuz, Persian Gulf. Petrol. Geosci. 17 (1), 101–107. https://doi.org/10.1144/1354-079309-799.

Agard, P., Omrani, J., Jolivet, L., Mouthereau, F., 2005. Convergence history across Zagros (Iran): constrains from collisional and earlier deformation. International Journal of Earth Scienes 98, 401–419. https://doi.org/10.1007/s00531-005-0481-4.

Agard, P., Omrani, J., Jolivet, L., Whitechuch, H., Vrielyck, B., Spakman, W., Monié, P., Meyer, B., Wortel, R., 2011. Zagros orogeny: a subduction-dominated process. Geol. Mag. 148 (5–6), 692–725.

Barrier, E., Vrielynck, B., 2008. Paleotectonic maps of the Middle East: atlas of 14 maps. In: Middle East Basin Evolution (MEBE), Programme. CGMW, Paris.

Beydoun, Z.R., 1991. Arabian Plate hydrocarbon geology and potential, a plate tectonic approach. AAPG Stud. Geol. 33, 77.

Berberian, M., King, G.C.P., 1981. Towards a paleogeography and tectonic evolution of Iran. Can. J. Earth Sci. 18, 210–265. https://doi.org/10.1139/e81-019.

Bozorgnia, H., Agah, S., 1973. Geological Information on Lar Block (Gr-360). National Iranian Oil Company Exploration and Production Affairs, p. 95.

Bowe, R.J., 1976. Geological Report Bandar Abbas Agreement Area, Iran (GR-5515-25). Phillips Petroleum Company Iran, p. 105.

Butler, R.W.H., Bond, C.E., Cooper, M.A., Watkins, H., 2018. Interpreting structural geometry in fold-thrust belts: why style matters. J. Struct. Geol. 114, 251–273. https://doi.org/10.1016/j.jsg.2018.06.019.

Callot, J.P., Jahani, S., Letuzey, J., 2007. The role of pre-existing diapirs in fold and thrust belt development. In: Lacombe, O., Lavè, J., Roure, F., Vergès, J. (Eds.), Thrust Belts and Foreland Basins. Springer, Berlin, pp. 309–325.

Callot, J.-P., Trocme, V., Letouzey, J., Albouy, E., Jahani, S., Sherkati, S., 2012. Pre-existing Salt Structures and the Folding of the Zagros Mountains, vol. 363. Geological Society of London Special Publication, pp. 545–561.

Carrera, N., Muñoz, J.A., Sàbat, F., Mon, R., Roca, E., 2006. The role of inversion tectonics in the structure of the Cordillera Oriental (NW Argentinean Andes). J. Struct. Geol. 28, 1921–1932. https://doi.org/10.1016/j.jsg.2006.07.006.

Coates, J., 1945. The construction of geological sections. Quarterly Journal Geological Mining Metallurgical Society (India) 1 (7), 1–11.

Coleman, R.G., 1981. Tectonic setting for ophiolite obduction in Oman. Journal of Geophysical research 86 (B4), 2497–2508. https://doi.org/10.1029/JB086iB04p02497.

Coleman, Alexander J., Jackson, Christopher A.-L., Duffy, Oliver B., Nikolinakou, Maria A., 2018. How, where, and when do radial faults grow near salt diapirs? Geology 46 (7), 655–658. https://doi.org/10.1130/G40338.1.

Dahlstrom, C.D.A., 1969. Balanced cross sections. Can. J. Earth Sci. 6, 743–757. https://doi.org/10.1139/e69-069.

Davis D., Suppe J., Dahlen F. A. (1983). Of fold-and-thrust belts and accretionary wedges. Journal of Geophysical Research: Solid Earth. Vol. 88, Issue B210, P. 1153-1172. https://doi.org/10.1029/JB088iB02p01153.

Davis, D.M., Engelder, T., 1985. The role of salt in fold-and-thrust belts. Tectonophysics 119 (Issues 1–4), 67–88. https://doi.org/10.1016/0040-1951(85)90033-2. ISSN 0040-1951.

De Böckh, H., Lees, G., Richardson, F.D.S., 1929. Contribution to the stratigraphy and tectonics of the Iranian ranges. In: Gregory, J.W. (Ed.), The Structure of Asia. Methuen, London, pp. 58–176.

Ezati Asl, M., Faghih, A., Mukherjee, S., Soleimany, B., 2019. Style and timing of salt movement in the Persian Gulf basin, offshore Iran: insights from halokinetic sequences adjacent to the Tonb-e-Bozorg salt diapir. J. Struct. Geol. (122), 116–132.

Falcon, N.L., 1969. In: Kent, P.E., Satterthwaite, G.E., Spencer, A.M. (Eds.), Problems of the Relationship between Surface Structure and Deep Displacements Illustrated by the Zagros Range, Special Publication 3, Time and Place in Orogeny: Geological Society of London, pp. 9–22.

Faqira, M., Rademakers, M., Kader, M.A., 2009. New insights into the Hercynian Orogeny, and their implications for the Paleozoic Hydrocarbon System in the Arabian Plate. GeoArabia 14 (3), 199–228.

Faridi, P., Rezaee, R., Piryaei, A.R., Masoodi, M., 2021. Halokinetic sequences as indicators of cenozoic diapiric growth: the Handun salt diapir (SE Zagros, bandar abbas). Geopersia 11 (2), 299–317. https://doi.org/10.22059/GEOPE.2021.313048.648581, 2021.

Farr, T.G., Rosen, A.P., Caro, E., Crippen, R., Duren, R., Hensley, S., Kobrick, M., Paller, M., Rodriguez, E., Roth, L., Seal, D., Shaffer, S., Shimada, J., Umland, J., Werner, M., Oskin, M., Burbank, D., Alsdorf, D., 2007. The Shuttle radar Topography mission. Rev. Geophys. 45. https://doi.org/10.1029/2005RG000183.

Frizon de Lamotte, D., Tavakoli-Shirazi, S., Leturmy, P., Averbuch, O., Mouchot, N., Raulin, C., Leparmentier, F., Blanpied, C., Ringenbach, J.C., 2013. Evidence for Late Devonian vertical movements and extensional deformation in northern Africa and Arabia: integration in the geodynamics of the Devonian world. Tectonics 32 (2), 107–122. https://doi.org/10.1002/tect.20007.

Gansser, A., 1960. Uber Schlammvulkane und Salzdome. Naturf. Gesell. Zurich Vierteljahrsschr 106 (1), 1–6.

Ghavidel-Syooki, M., Popov, L.E., Álvaro, J.J., Pour, M.G., Tolmacheva, T.Y., Ehsani, M. H., 2014. Dapingian-lower darriwilian (ordovician) stratigraphic gap in the faraghan mountains, Zagros ranges, south-eastern Iran. Bull. Geosci. 89 (4), 679–706.

Gill, W.D., 1953. Construction of geological cross-sections of folds with steep-limb attenuation. AmericanAssociation of PetroleumGeologists. Bulletin 37, 2389–2406.

Giles, K.A., Rowan, M.G., 2012. Concepts in halokinetic-sequence deformation and stratigraphy. Salt Tectonics, Sediments and Prospectivity 363, 7–31. https://doi.org/10.1144/SP363.2. Geological Society, London, Special Publications.

Groshong, R.H., 2006. 3D Structural Geology: A Practical Guide to Quantitative Surface and Subsurface Map Interpretation. Springer-Verlag, Berlin, Heidelberg.

Harrison, M.R.J.V., 1931. Salt domes in persia. In: Symposium on Salt Domes. 17. Inst. Petroleum Technologists Journal, pp. 300–320.

Hassanpour, J., Muñoz, Josep Anton, Ali, Yassaghi, Ferrer, Oriol, Jahani, Salman, Santolaria, Pablo, SeyedAli, Seyed Mohsen, 2021. Impact of salt layers interaction on the salt flow kinematics and diapirism in the Eastern Persian Gulf, Iran: constraints from seismic interpretation, sequential restoration, and physical modelling. Tectonophysics 811, 228887. https://doi.org/10.1016/j.tecto.2021.228887. ISSN 0040-1951.

Hinsch, R., Vögele, Martin, Gharabeigli, Gholamreza, Bretis, Bernhard, Tari, Gabor, 2022. Uncertainties of balanced sections and the role of basement in the southern Fars area, Iran. J. Struct. Geol. 163, 104686. https://doi.org/10.1016/j.jsg.2022.104686. ISSN 0191-8141.

Husseini, M.I., 1988. The Arabian lnfracambrian extensional system. Tectonophysics 148, 93–103.

Husseini, M.I., Husseini, I.S., 1990. Origin of the infracambrian salt basins of the Middle East. In: Classic Petroleum Provinces, 279. Geological Society Special Publication, pp. 279–292. No 50.

Husseini, M.I., 2000a. Origin of the Arabian plate structures: amar collission and Najd Rift. GeoArabia 5 (4), 527–542.

Humphris Jr., C.C., 1978. Salt Movement on Continental Slope, Northern Gulf of Mexico. A. H.
Humphris Jr., C.C., 1979. Salt movement in continental slope, northern Gulf of Mexico. AAPG (Am. Assoc. Pet. Geol.) Bull. 63, 782–798.
James, G.A., Wynd, J.G., 1965. Stratigraphic nomenclature of Iranian oil Consortium agreement area. AAPG (Am. Assoc. Pet. Geol.) Bull. 49, 2182–2245.
Jahani, S., Callot, J.P., Letouzey, J., Frizon De Lamotte, D., 2009. The eastern termination of the Zagros Fold-and-Thrust Belt, Iran: structures, evolution, and relationships between salt plugs, folding, and faulting. Tectonics 28 (6), TC6004. https://doi.org/10.1029/2008TC002418.
Jahani, S., Hassanpour, J., Mohammadi-Firouz, S., Letouzey, J., Frizon de Lamotte, D., Alavi, S.A., Soleimany, B., 2017. Salt tectonics and tear faulting in the central part of the Zagros Fold-Thrust Belt, Iran. Mar. Pet. Geol. 86, 426–446.
Jackson, M.P.A., Vendeville, B.C., 1994. Regional extension as a geologic trigger for diapirism. Geological Society American Bull 106, 57–73.
Khadivi, S., Mouthereau, F., Barbarand, J., Adatte, T., Lacombe, O., 2012. Constraints on palaeodrainage evolution induced by uplift and exhumation on the southern flank of the Zagros-Iranian plateau. J. Geol. Soc. 169 (1), 83–97.
Kent, P.E., 1958. Recent studies of South Persian salt plugs. AAPG 42, 2951–2972.
Kent, P.E., 1970. The salt plugs of the Persian Gulf region. Trans. Leic. Literao Philos. Soc. 64, 65–88.
Koop, W.J., Stoneley, R., Ridd, M.F., Murphy, R.W., Osmaston, M.F., Kholief, M.M., 1982. Subsidence History of the Middle East Zagros Basin, Permian to Recent [and Discussion], vol. 305. Philosofical Transaction of the Royal Society of London A, pp. 149–168. https://doi.org/10.1098/rsta.1982.0031.
Langenberg, W., Charlesworth, H., La Riviere, A., 1987. Computer-constructed cross-sections of the Morcles nappe. Eclogae Geol. Helv. 80 (3), 655–667.
Lees, G.M., 1931. Salt - some depositional and deformational problems. In: Symposium on Salt Domes. 17. Institute of Petroleum Technologists Journal, pp. 259–280.
Leturmy, P., Robin, C., 2010. Tectonic and Stratigraphic Evolution of Zagros and Makran during the Mesozoic–Cenozoic, vol. 330. Geological Society, London, Special Publications, pp. 121–138. https://doi.org/10.1144/SP330.7.
Mallet, J.L., 1992. GOCAD: a computer aided design program for geological applications. In: Turner, A.K. (Ed.), Three-Dimensional Modeling with Geoscientific Information Systems, NATO ASI Series, vol. 354. Springer, Dordrecht. https://doi.org/10.1007/978-94-011-2556-7_11.
Marshak, S., Woodward, N., 1988. Introduction to cross-section balancing. In: Marshak, S., Mitra, G. (Eds.), Basic Methods of Structural Geology. Prentice Hall, Englewood Cliffs, New Jersey, 303–302.
McQuarrie, N., Stock, J.M., Verdel, C., Wernicke, B.P., 2003. Cenozoic evolution of Neotethys and implications for the causes of plate motions. Geophys. Res. Lett. 30 (20), 2036. https://doi.org/10.1029/2003GL017992.
McQuarrie, N., van Hinsbergen, D.J., 2013. Retrodeforming the Arabia-Eurasia collision zone: age of collision versus magnitude of continental subduction. Geology 41, 315–318. https://doi.org/10.1130/G33591.1.
Mitra, S., 1992. Balanced structural interpretations in fold and thrust belts. In: Mitra, S., Fisher, G.W. (Eds.), Structural Geology of Fold and Thrust Belts. Johns Hopkins University Press, Maryland, pp. 53–77.
Molinaro, M., Leturmy, P., Guezou, J.-C., Frizon de Lamotte, D., Eshraghi, S.A., 2005. The structure and kinematics of the southeastern Zagros fold-thrust belt, Iran: from thin-skinned to thick-skinned tectonics. Tectonics 24, TC3007. https://doi.org/10.1029/2004TC001633.
Motiei, H., 1995. Petroleum Geology of Zagros, 1 and 2 (In Farsi). Geological Survey of Iran, Tehran.
Mouthereau, F., Lacombe, O., Vergés, J., 2012. Building the Zagros collisional orogen: timing, strain distribution and the dynamics of Arabia/Eurasia plate convergence. Tectonophysics 532, 27–60. https://doi.org/10.1016/j.tecto.2012.01.022.
Mouthereau, F., Tensi, J., Bellahsen, N., Lacombe, O., de Boisgrollier, T., Kargar, S., 2007. Tertiary sequence of deformation in a thin-skinned/thick-skinned collision belt: the Zagros Folded Belt (Fars, Iran). Tectonics 26, TC5006. https://doi.org/10.1029/2007TC002098.
Nabavi, S.T., Ruh, J.B., 2023. Hybrid thrust sequences–a new structural perspective. J. Asian Earth Sci. 253. https://doi.org/10.1016/j.jseaes.2023.105701.
Nikolinakou, M.A., Flemings, P.B., Hudec, M.R., 2014. Modeling stress evolution around a rising salt diapir. Mar. Petrol. Geol. 51, 230–238. https://doi.org/10.1016/j.marpetgeo.2013.11.021.
Nissen, E., Jackson, J., Jahani, S., Tatar, M., 2014. Zagros "phantom earthquakes" reassessed - the interplay of seismicity and deep salt flow in the Simply Folded Belt? J. Geophys. Res. Solid Earth 119 (4), 3561–3583.
Nissen, E., Tatar, M., Jackson, J.A., Allen, M.B., 2011. New views on earthquake faulting in the Zagros fold-and-thrust belt of Iran. Geophys. J. Int. 186 (3), 928–944.
Orang, K., Hossein, M., Azadikhah, A., Royatvand, M., 2017. Structural framework and tectono-stratigraphic evolution of the easten Persian Gulf, offshore Iran. Mar. Petrol. Geol. 91, 89–107. https://doi.org/10.1016/j.marpetgeo.2017.12.014.
Perotti, C., Chiariotti, L., Bresciani, L., Cattaneo, L., Toscani, G., 2016. Evolution and timing of salt diapirism in the Iranian sector of the Persian Gulf. Tectonophysics 679, 180–198.
Peacock, D.C., Banks, G.J., 2020. Basement highs: definitions, characterisation and origins. Basin Res. 32 (6), 1685–1710.
Pirouz, M., Simpson, G., Chiaradia, M., 2015. Constraint on foreland basin migration in the Zagros mountain belt using Sr isotope stratigraphy. Basin Res. 27, 714–728.
Player, R.A., 1969. The Hormuz Salt Plugs of Southern Iran. Ph.D. thesis, Reading Universiy, p. 300.
Rahmani, Z., Vaziri-Moghaddam, H., Taheri, A., 2010. Facies distribution and palaeoecology of the Guri member of the mishan formation. In: Lar Area, Fars Province, SW Iran. Iranian Journal of Science and Technology. Transaction A, vol. 34, pp. 257–266. A3.
Rezae, P., 2014. Depositional evolution and sediment facies pattern of the tertiary basin in southern Zagros, south Iran. Asian J. Earth Sci. 7 (2), 27–39.
Richardson, R.K., 1926. Die geologie und die salzdome im südwetlichen teile des Persischen Golfes: Verhandlunger der Naturhistorischen, vol. 15. Medzin Verein Heidelberg, p. 51.
Ricou, L.E., Braud, J., Brunn, J.H., 1977. Le Zagros. Mem. Soc. Geol. Fr. 8, 33–52.
Rowan, M.G., 1993. A systematic technique for the sequential restoration of salt structures. Tectonophysics 228, 331–348. https://doi.org/10.1016/0040-1951(93)90347-M.
Rowan, M.G., 2002. Salt-related accommodation in the Gulf of Mexico deepwater: withdrawal or inflation, autochthonous or allochthonous? Gulf Coast Association of Geological Societies Transactions 52, 861–869.
Rowan, M.G., Lawton, T.F., Giles, K.A., Ratliff, R.A., 2003. Near-salt deformation in La Popa basin, Mexico, and the northern Gulf of Mexico: a general model for passive diapirism. AAPG (Am. Assoc. Pet. Geol.) Bull. 87 (5), 733–756.
Rowan, M.G., Muñoz, J.A., Giles, K.A., Roca, E., Hearon IV, T.E., Fiduk, J.C., Ferrer, O., Fischer, M.P., 2020. Folding and fracturing of rocks adjacent to salt diapirs. J. Struct. Geol. 141, 104187.
Ruh, J.B., Kaus, B.J., Burg, J.P., 2012. Numerical investigation of deformation mechanics in fold-and-thrust belts: influence of rheology of single and multiple décollements. Tectonics 31 (3). https://doi.org/10.1029/2011TC003047.
Saberi, M.H., Rabbani, A.R., Ghavidel-syooki, M., 2016. Hydrocarbon potential and palynological study of the latest ordovician-easrliest silurian source rock (sarchahan formation) in the Zagros mountains, southern Iran. Mar. Petrol. Geol. 71, 12–25.
Santolaria, P., Ferrer, O., Rowan, M.G., Snidero, M., Carrera, N., Granado, P., et al., 2021a. Influence of preexisting salt diapirs during thrust wedge evolution and secondary welding: insights from analog modeling. J. Struct. Geol. 149, 104374. https://doi.org/10.1016/j.jsg.2021.104374.
Santolaria, P., Granado, P., Carrera, N., Schneider, C.L., Ferrer, O., Snidero, M., et al., 2021b. From downbuilding to contractional reactivation of salt-sediment systems: insights from analog modeling. Tectonophysics 918, 229078. https://doi.org/10.1016/j.tecto.2021.229078.
Saura, E., et al., 2011. Basin architecture and growth folding of the NW Zagros early foreland basin during the Late Cretaceous and early Tertiary. J. Geol. Soc. 168, 235–250. https://doi.org/10.1144/0016-76492010-092. London.
Searle, M.P., Cherry, A.G., Ali, M.Y., cooper, D.J.W., 2014. Tectonics of the Musandam Peninsula and northern Oman Mountains: from ophiolite obduction to continental collision. GeoArabia 19, 135–174.
Sepehr, M., Cosgrove, J.W., 2004. Structural framework of the Zagros fold–thrust belt, Iran. Mar. Pet. Geol. 21 (7), 829–843. https://doi.org/10.1016/j.marpetgeo.2003.07.006.
Snidero, M., Amilibia, A., Gratacos, O., Blanc, E.J.P., Muñoz, J.A., 2011. The 3D reconstruction of geological structures based on remote sensing data: example from the Anaran anticline, Lurestan province, Zagros fold and thrust belt, Iran. J. Geol. Soc. https://doi.org/10.1144/0016-76492010-107.
Snidero, M., 2021. Role of Inheritances in Shaping the Zagros Fold and Thrust Belt (Doctoral Dissertation). University of Naples Federico II. Retrieved from. https://www.researchgate.net/profile/Marco-Snidero/publications.
Snidero, M., Muñoz, J.A., Carrera, N., Butillé, M., Mencos, J., Motamedi, H., et al., 2019. Temporal evolution of the Darmadan salt diapir, eastern Fars region. Iran. Tectonophysics 766, 115–130. https://doi.org/10.1016/j.tecto.2019.06.006.
Snidero, M., Carrera, M.N., Mencos, J., Butillé, M., Granado, P., Tavani, S., Lopez-Mir, B., Sàbat, F., Muñoz, J.A., 2020. Diapir kinematics in a multi-layer salt system from the eastern Persian Gulf. Mar. Petrol. Geol. 117, 104402. https://doi.org/10.1016/j.marpetgeo.2020.104402. ISSN 0264-8172.
Snidero, M., 2023. Supporting data for the structural evolution of the Handun salt diapir, Zagros fold and thrust belt. figshare. Dataset. https://doi.org/10.6084/m9.figshare.24039132.
Stewart, S.A., 2017. Hormuz Salt distribution and influence on structural style in NE Saudi Arabia. Petrol. Geosci. https://doi.org/10.1144/petgeo2017-011.
Stöcklin, J., 1968. Structural history and tectonics of Iran: a review. AAPG (Am. Assoc. Pet. Geol.) Bull. 52, 1229–1258.
Stoesser, D.B., Camp, V.E., 1985. Pan-African microplate accretion of the Arabian shield. GSA Bulletin 96, 817–826.
Stoneley, R., 1981. The geology of the kuh-e dalneshin area of southern Iran, and its bearing on the evolution of southern tethys. J. Geol. Soc. 138, 509–526. https://doi.org/10.1144/gsjgs.138.5.0509.
Suppe, J., 1985. Principles of Structural Geology. Prentice-Hall, Englewood Cliffs, NJ.
Tavakoli, S., Frizon de Lamotte, D., Wrobel-Daveau, J.-C., Ringenbach, J.-C., 2013. Pre-Permian uplift and diffuse extensional deformation in the High Zagros Belt (Iran): integration in the geodynamic evolution of the Arabian plate. Arab. J. Geosci. 6 (7), 2329–2342. https://doi.org/10.1007/s12517-012-0542-5.
Tavani, S., Arbués, P., Snidero, M., Carrera García de Cortázar, N., Muñoz, J.A., 2011. Open Plot Project: an open-source toolkit for 3-D structural data analysis. Solid Earth 2, 53–63. https://doi.org/10.5194/se-2-53-2011.
Tavani, S., Parente, M., Puzone, F., Corradetti, A., Gharabeigli, G., Valinejad, M., Morsalnejad, D., Mazzoli, S., 2018. The seismogenic fault system of the 2017 Mw 7.3 Iran-Iraq earthquake: constraints from surface and subsurface data, crosssection balancing and restoration. Solid Earth 9, 821–831. https://doi.org/10.5194/se-9-821-2018.
Tavani, S., Camanni, G., Nappo, M., Snidero, M., Ascione, A., Valente, E., Gholamreza, G., Davoud, M., Mazzoli, S., 2020. The Mountain Front Flexure in the Lurestan region of the Zagros belt: crustal architecture and role of structural inheritances. J. Struct. Geol., 104022 https://doi.org/10.1016/j.jsg.2020.104022.

Vendeville, B.C., Jackson, M.P.A., 1991. The Rise of Diapirs during Thin-Skinned Extension. Bureau of Economic Geology, The University of Texas at Austin, Austin, TX 78713, USA.

Vergés, J., Saura, E., Casciello, E., Fernàndez, M., Villaseñor, A., Jiménez-Munt, I., García-Castellanos, D., 2011. Crustal-scale cross-sections across the NW Zagros belt: implications for the Arabian margin reconstruction. Geol. Mag. 148, 739–761. https://doi.org/10.1017/S0016756811000331.

Zamanzadeh, S.M., Amini, A., Ghavidel Syooki, M., 2009. Sequence stratigraphic controls on early-diagenetic carbonate cementation of shallow marine clastic sediments (the Devonian Zakeen Formation, southern Zagros, Iran). Geosci. J. 13 (1), 31–57.

Ziegler, M.A., 2001. Late permian to holocene paleofacies evolution of the Arabian plate and its hydrocarbon occurrences. GeoArabia 6, 445–504.